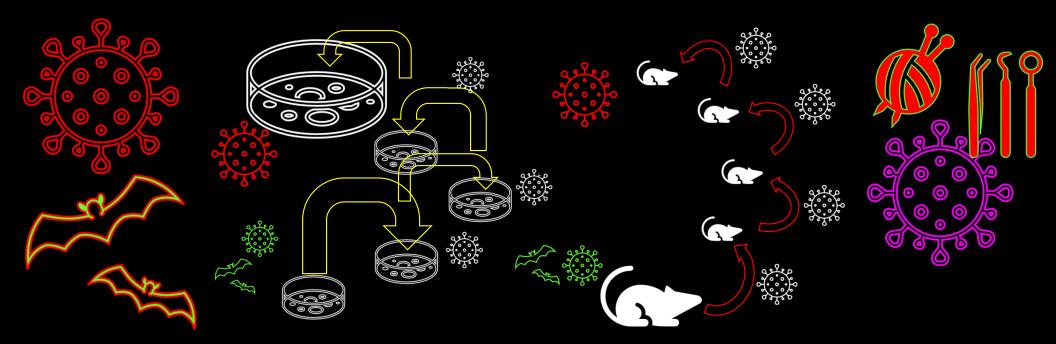


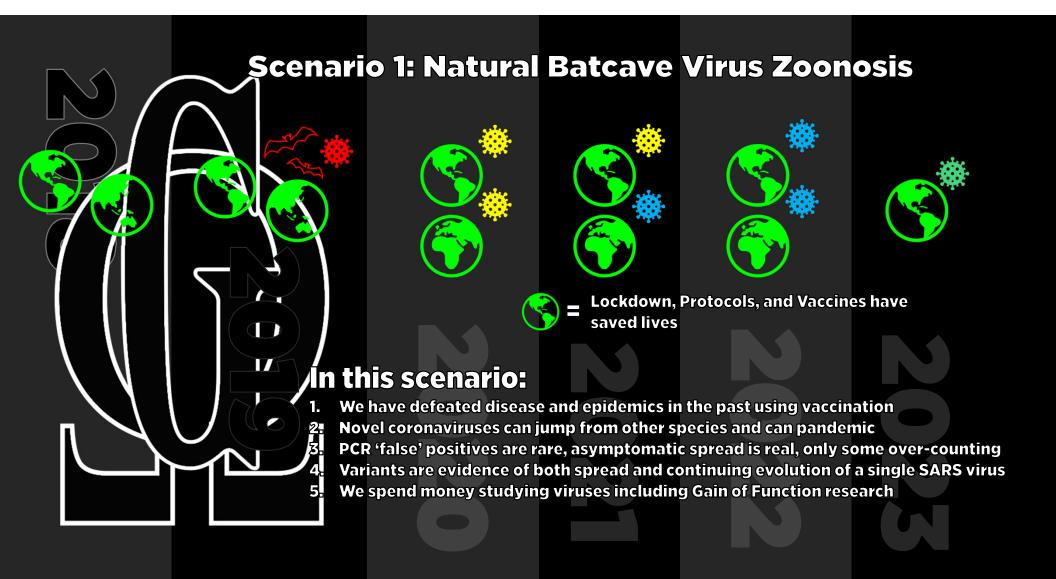
The TV and algorithms have told us that coronaviruses have pandemic potential

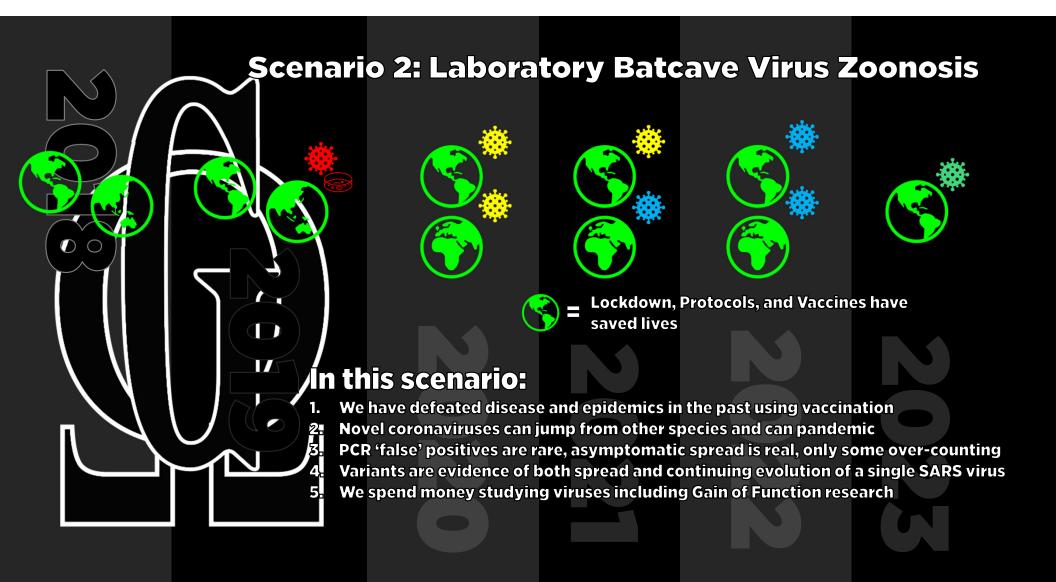
This potential can be accessed through cell culture, animal passage, and human engineering

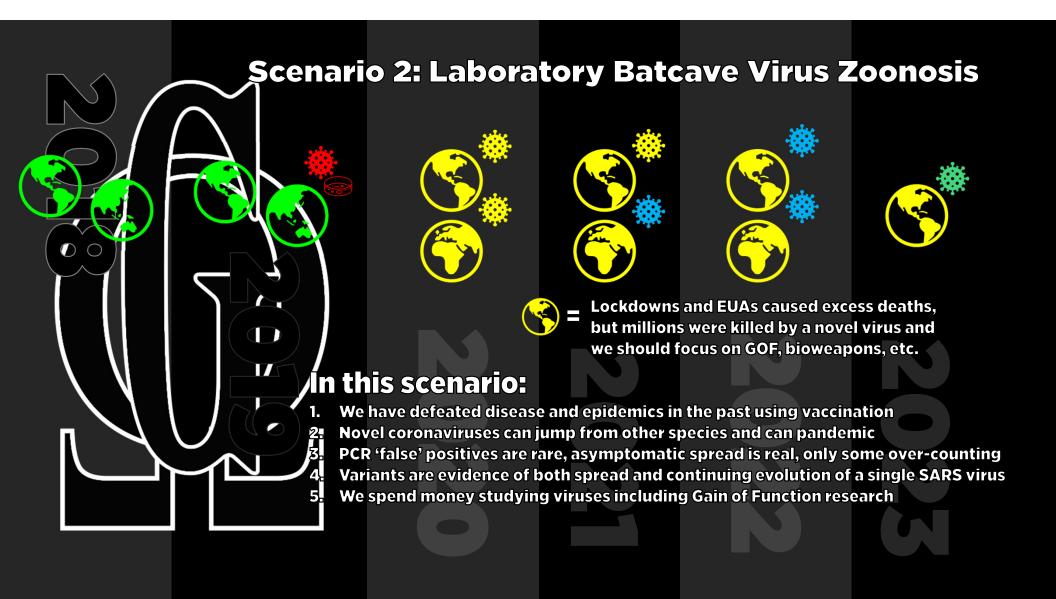
Therefore, the global population must surrender sovereignty to the WHO

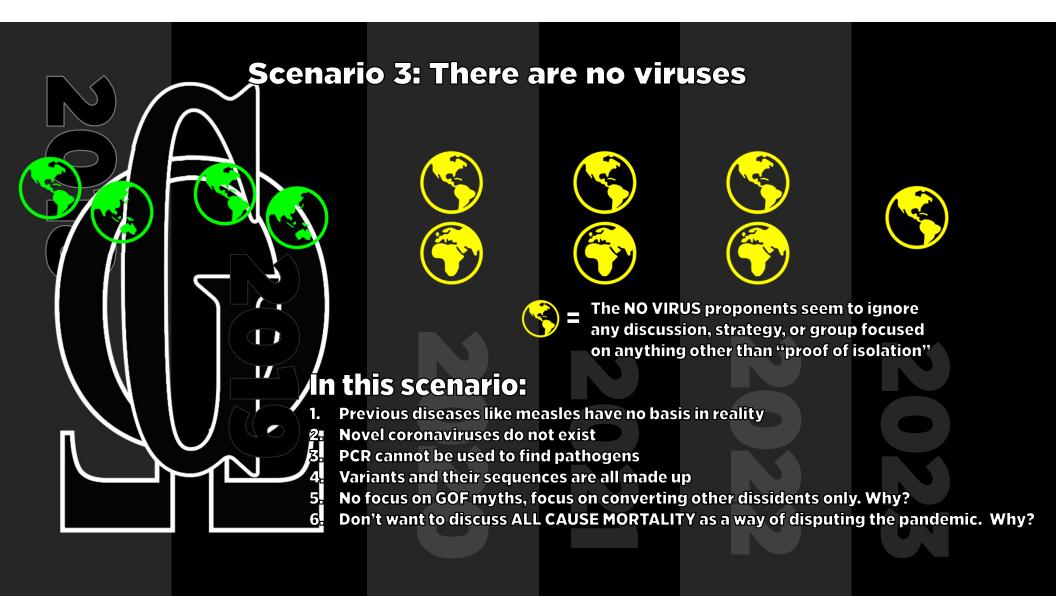


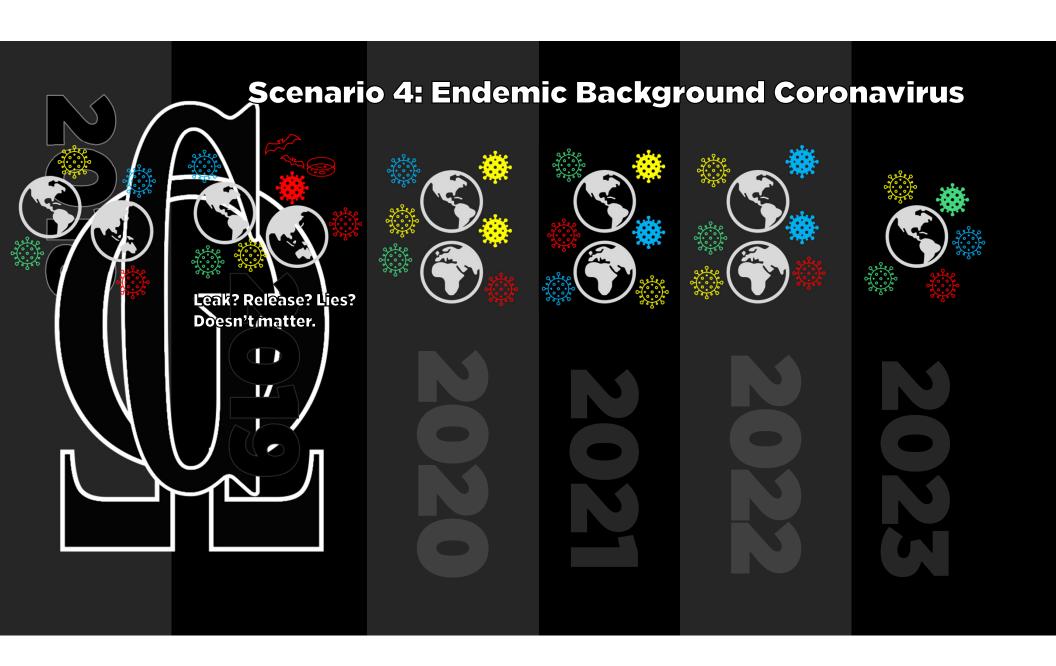
To coerce a surrender of individual sovereignty and a global fundamental inversion of human rights from freedom to fascism

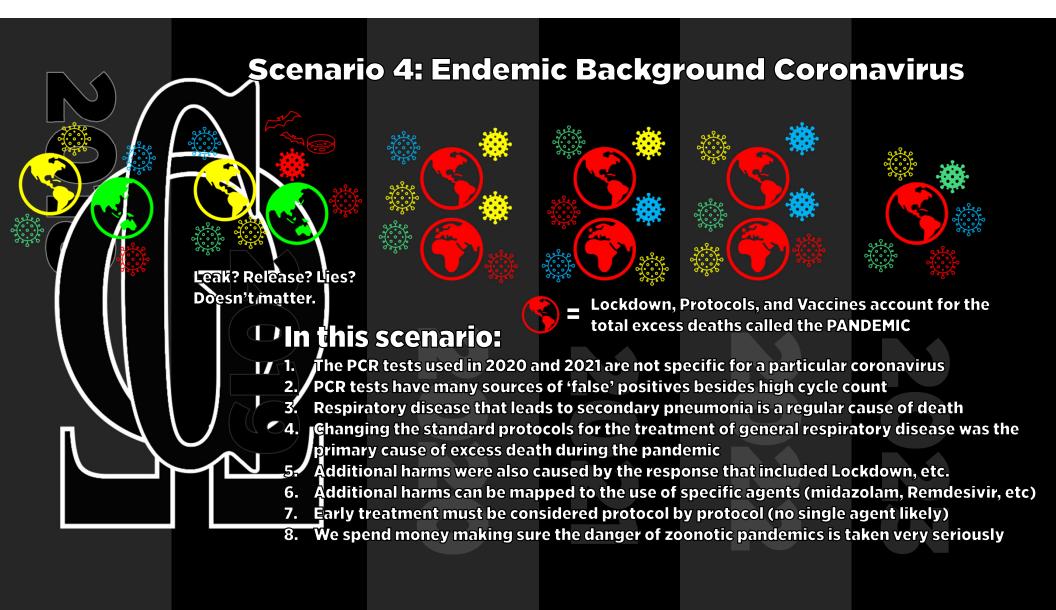












■ TO TAL DEATHS

NUM COVID-19 DEATHS

NUM PNEUMONIA DEATHS

NUM INFLUENZA DEATHS

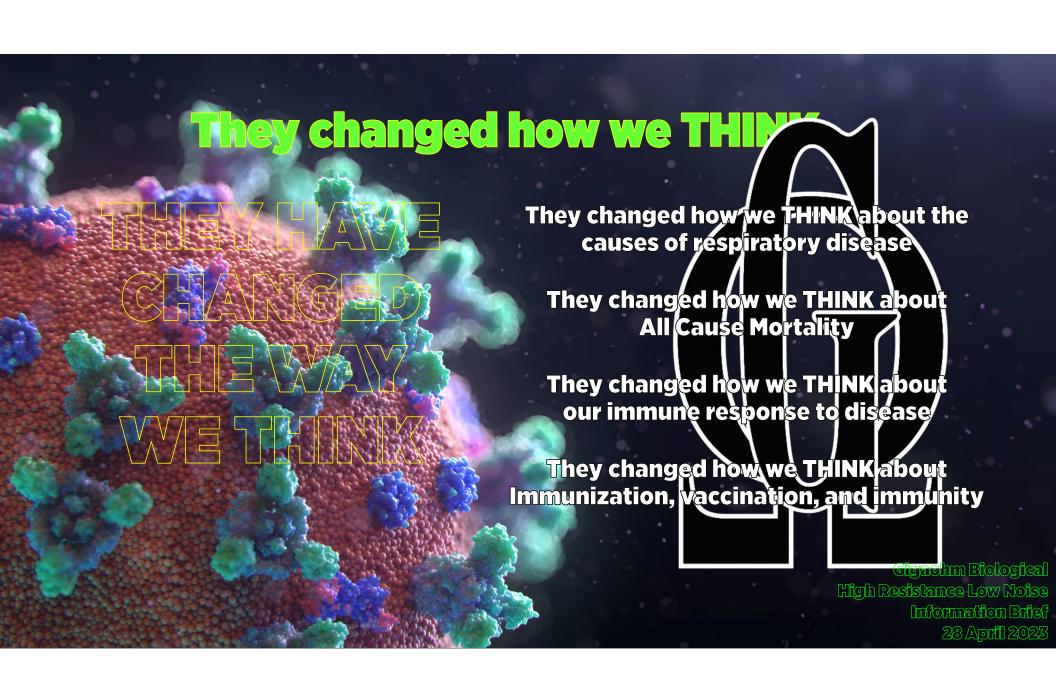
₁₀ Hypothesis:

The WHO declared a pandemic of a DANGEROUS NOVEL virus—said to be detectable by non-specific PCR test for RNA viruses applied to low prevalence populations (high percentage false positives and endemic background signal) and intentionally correlated with poor or detrimental health protocols through financial incentives—that enabled a larger percentage of all cause mortality than PnI (pneumonia and influenza) to be prioritized as a national security threat composed of vaccine preventable deaths. The US was ready with a plan to respond to a coronavirus pandemic, and that plan is in motion.

A NIAID funded infectious DNA/RNA infectious clone of a CoV may or may not be involved in the initial biological incident(s), but a natural CoV swarm cannot sustain a pandemic.

The goal is the total surrender of individual sovereignty and enforcement of a global fundamental inversion from basic human rights to basic granted

permissions



They changed how we THINK

They changed how we THINK about the Human Coronavirus Swarm

They changed how we THINK about All Cause Mortality

They changed how we THINK about our immune response to a respiratory virus

They changed how we THINK about Immunization, vaccination, and immunity

They ventilated to prevent spread Shutting down schools hurt kids Masking hurt kids Social distancing hurt families and the communities in which they exist

Cigachm Biological High Resistance Low Noise Information Brief 23 April 2023

Mind & Brain Environment Technology Space & Physics Video Podcasts

a

Save 25% on Digital

Shop Now

It's not a matter of what is true that counts but a matter of what is perceived to be true

PUBLIC HEALTH

5 Things We've Learned from **COVID** in Three Years

The World Health Organization declared the COVID outbreak a pandemic three years ago. Here's what's changed since then

By Stephanie Pappas on March 13, 2023





People visit the In America: Remember public art installation near the Washington Monument in Washington, D.C., on September 20, 2021. The installation commemorates all the Americans who have died because of COVID and is a concept by artist Suzanne Brennan Firstenberg. It includes more than 650,000 small plastic flags, some with personal messages to those who have died, planted in 20 acres of the National Mall. Credit: Kent Nishimura/Los Angeles Times/Getty Images

READ THIS NEXT

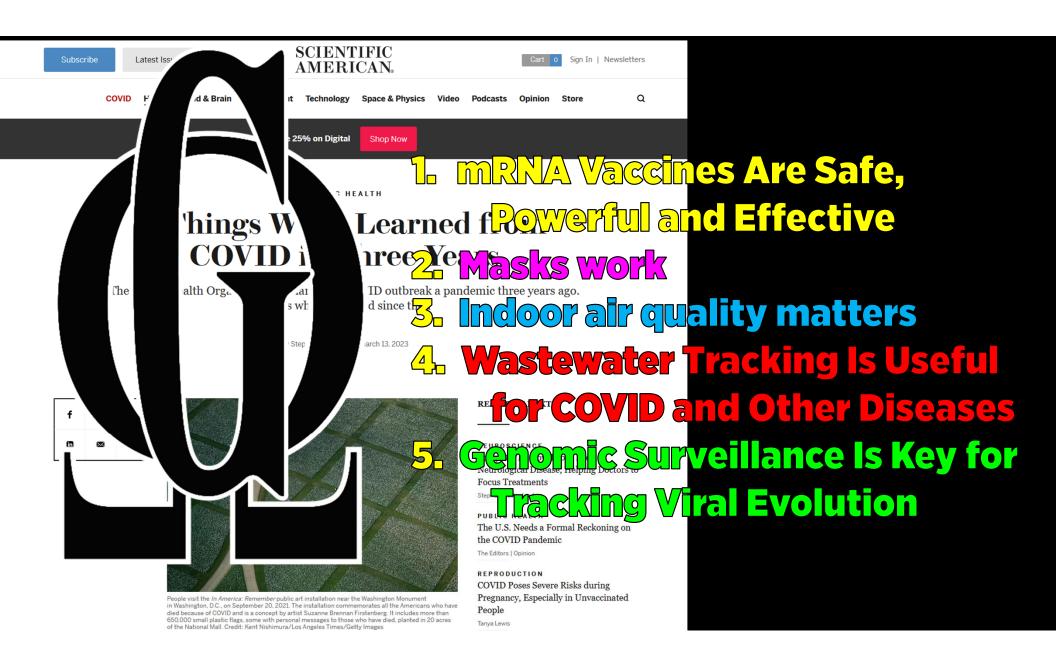
NEUROSCIENCE Long COVID Now Looks like a Neurological Disease, Helping Doctors to Focus Treatments

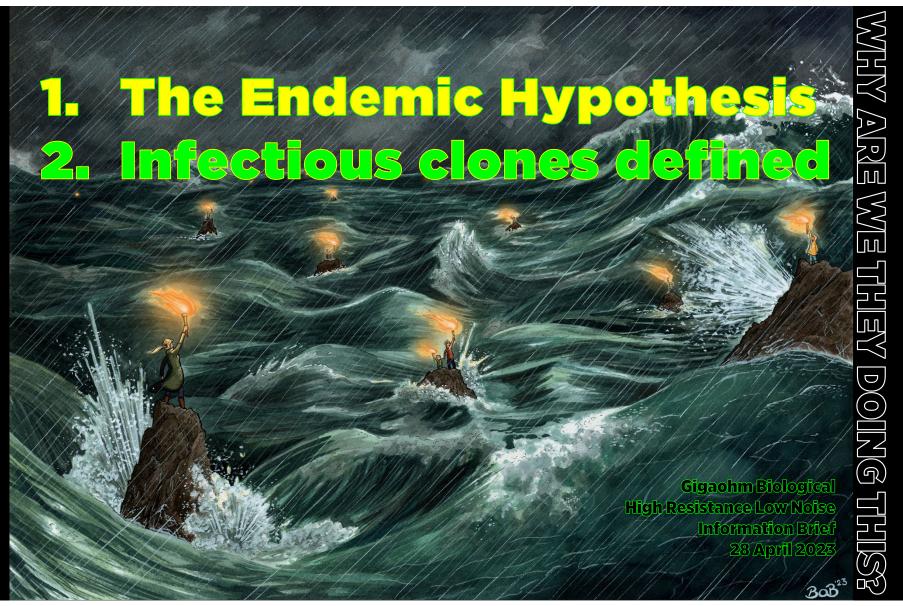
Stephani Sutherland

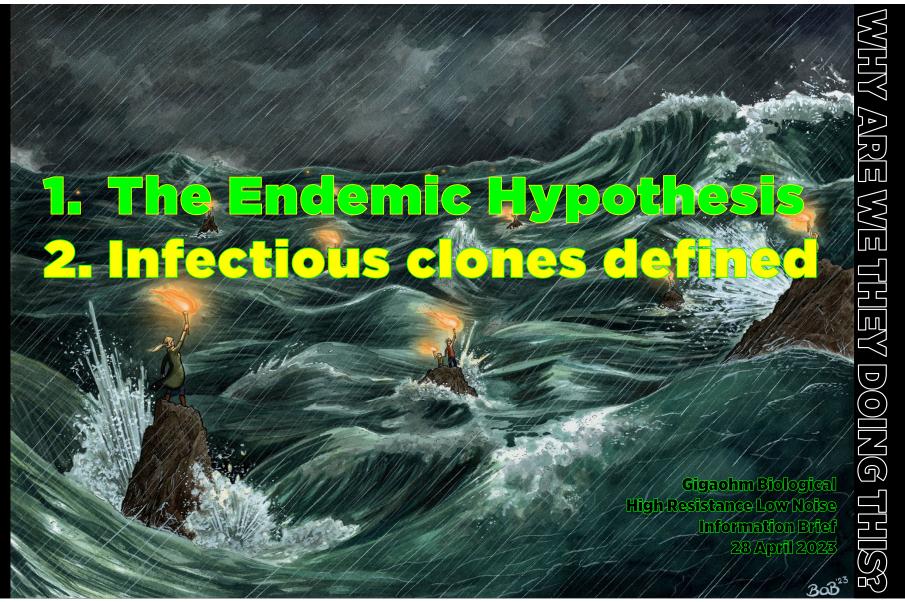
PUBLIC HEALTH The U.S. Needs a Formal Reckoning on the COVID Pandemic

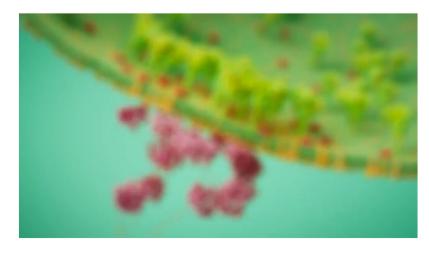
The Editors | Opinion

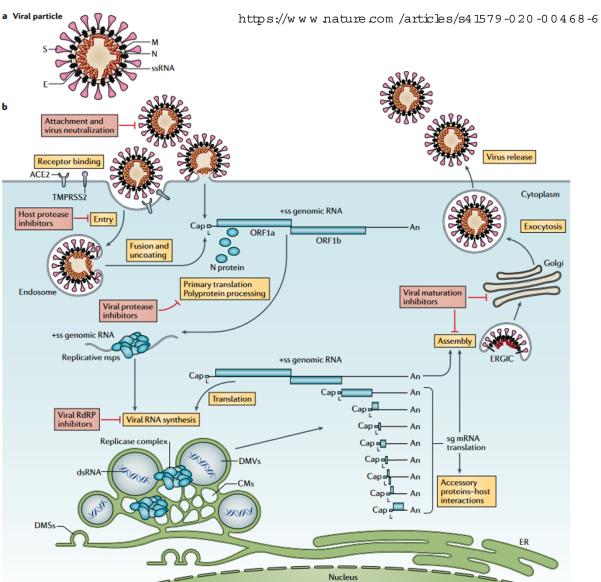
REPRODUCTION COVID Poses Severe Risks during Pregnancy, Especially in Unvaccinated People



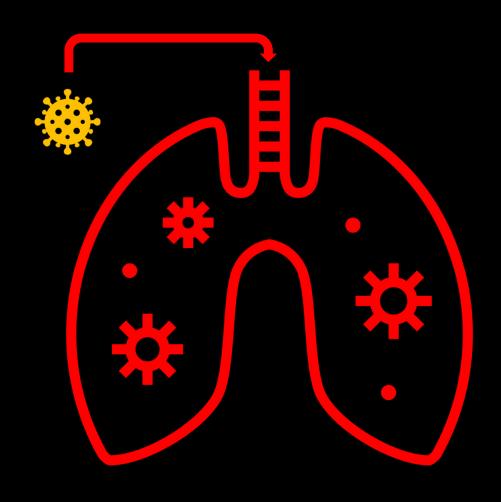




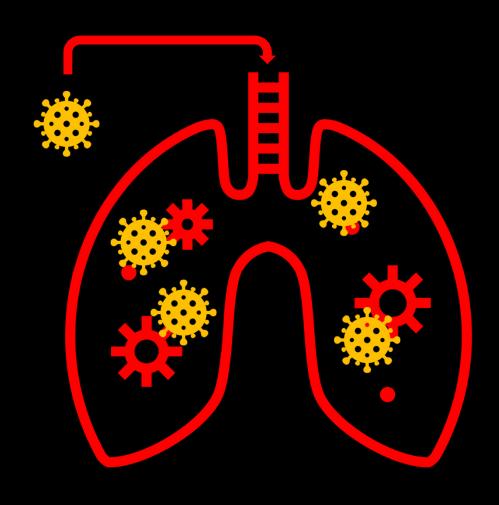


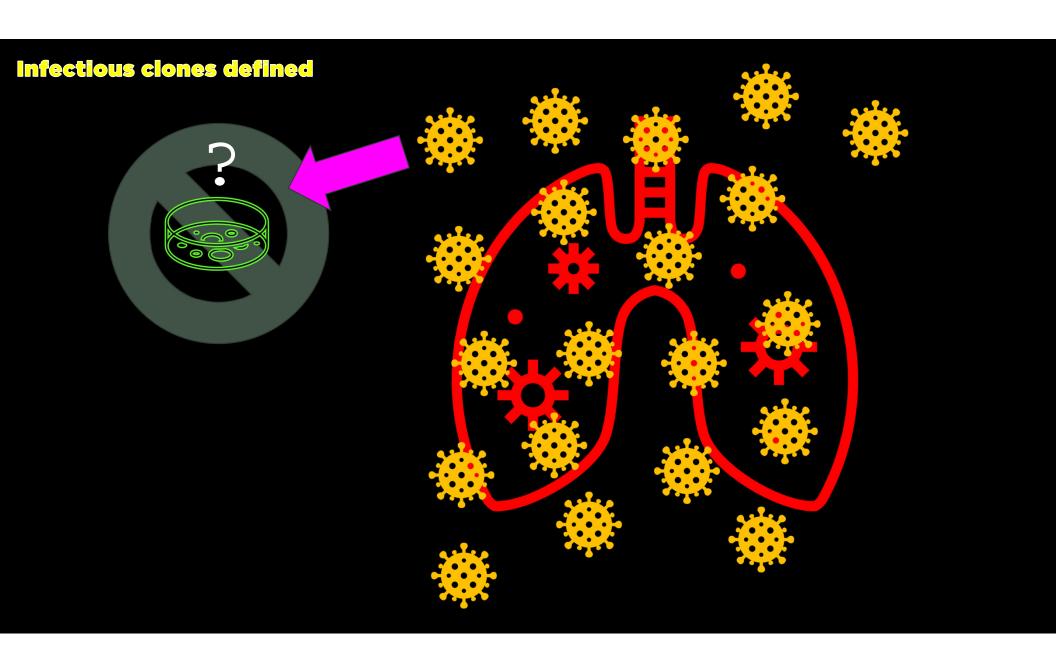


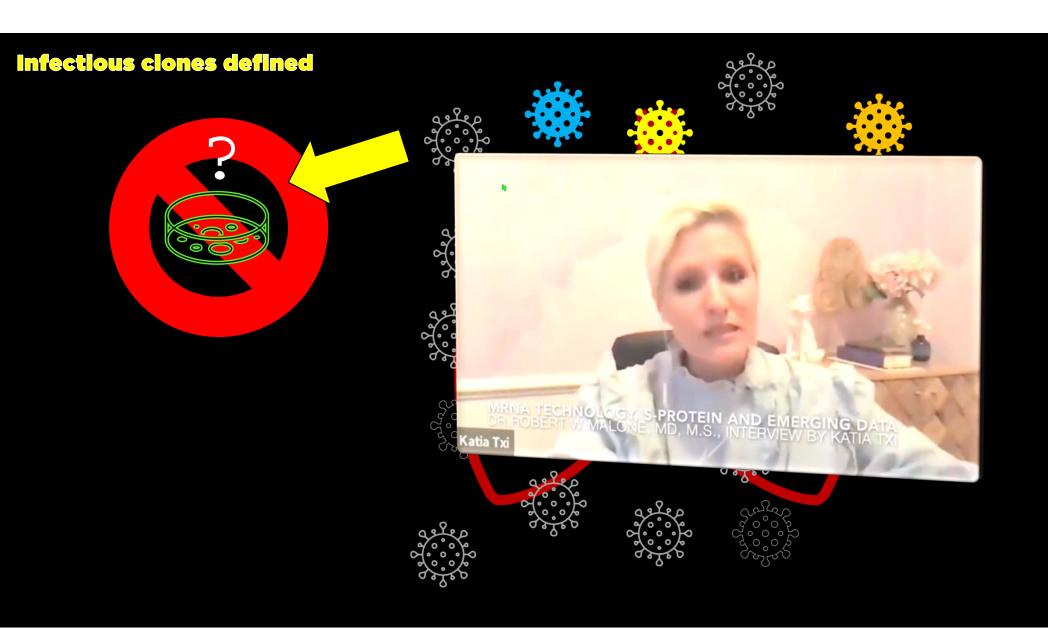
Infectious ciones defined

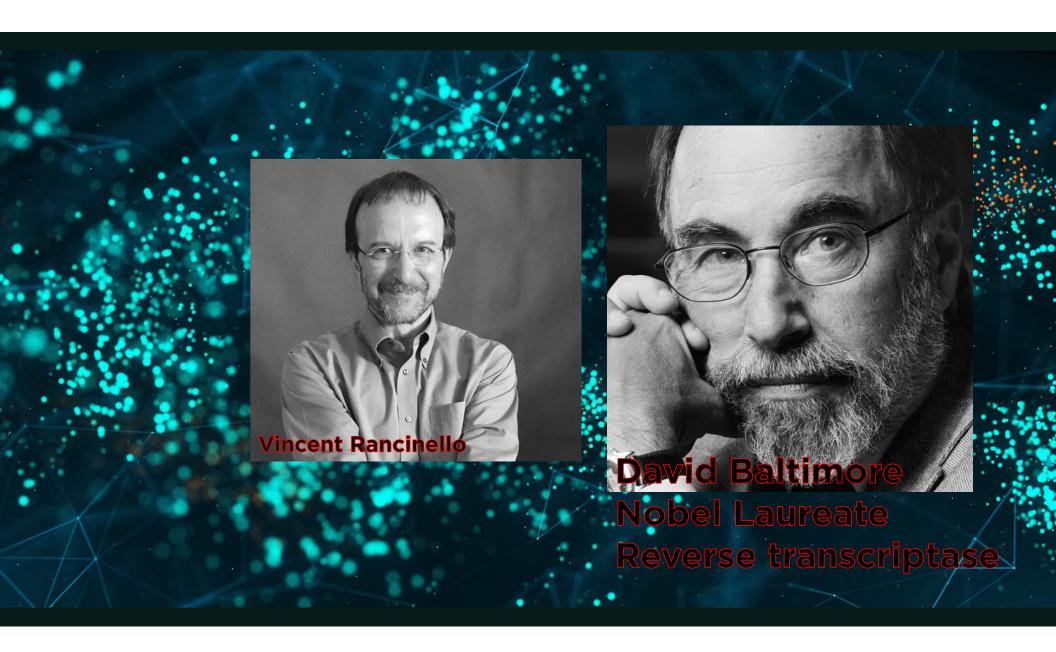


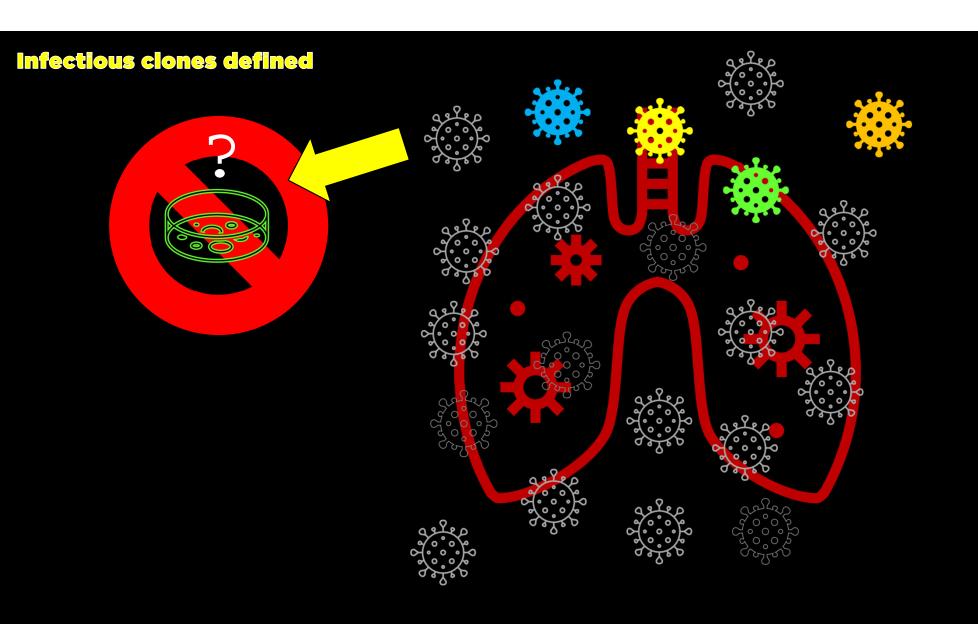
Infectious ciones defined

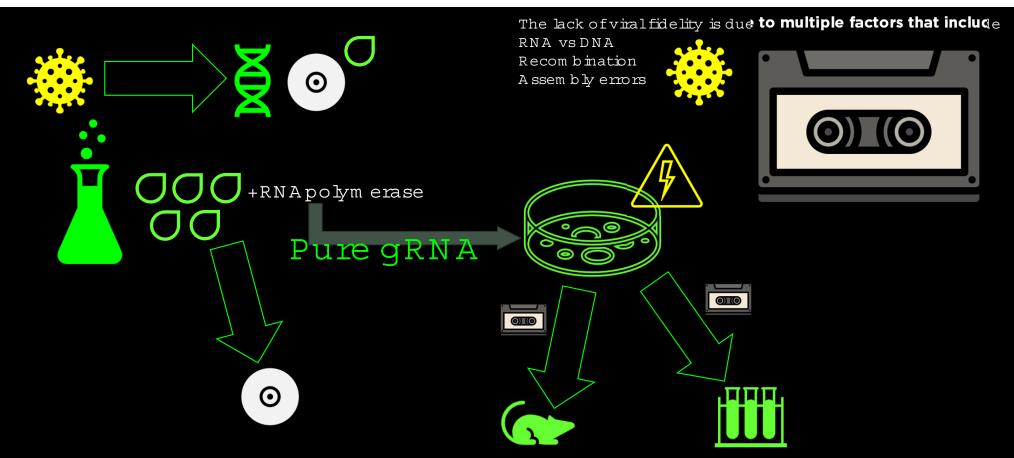




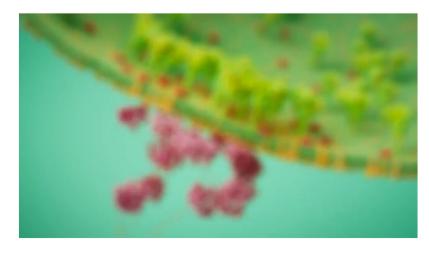


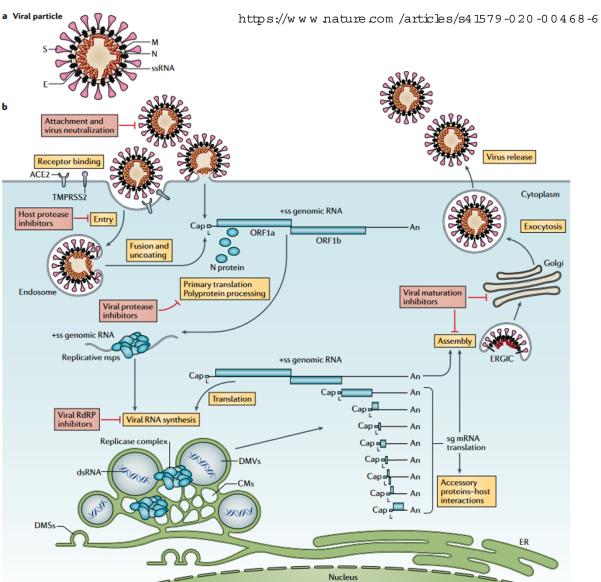


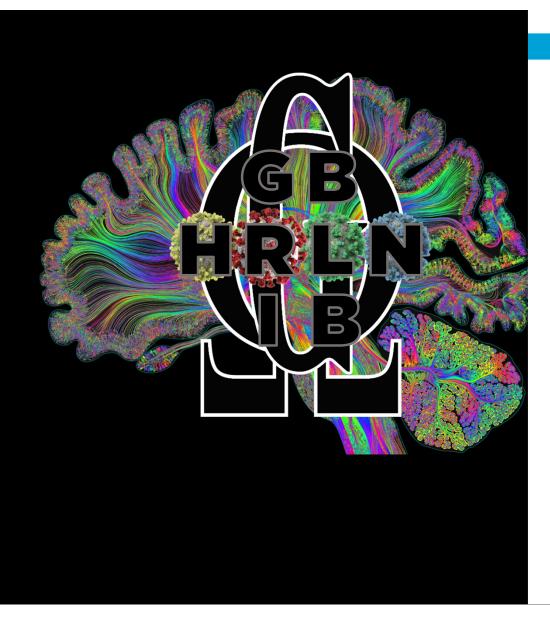




cDNAs are used in this exact manner to create the mRNA tranfections.
The cDNA contam ination in the transfections is from this exact process.







CelPress

Cell

Resource

The Architecture of SARS-CoV-2 Transcriptome

Dongwan Kim, ^{1,2} Joo-Yeon Lee,³ Jeong-Sun Yang,³ Jun Won Kim,³ V. Narry Kim, ^{1,2,4,*} and Hyeshik Chang ^{1,2,*} ¹Center for RNA Research, Institute for Basic Science (IBS), Seoul 08826, Republic of Korea

²School of Biological Sciences, Seoul National University, Seoul 08826, Republic of Korea

³Korea National Institute of Health, Korea Centers for Disease Control and Prevention, Osong 28159, Republic of Korea ⁴Lead Contact

*Correspondence: narrykim@snu.ac.kr (V.N.K.), hyeshik@snu.ac.kr (H.C.)

https://doi.org/10.1016/j.cell.2020.04.011

SARS-CoV-2 is a betacoronavirus responsible for the COVID-19 pandemic. Although the SARS-CoV-2 genome was reported recently, its transcriptomic architecture is unknown. Utilizing two complementary sequencing techniques, we present a high-resolution map of the SARS-CoV-2 transcriptome and epitranscriptome. DNA nanoball sequencing shows that the transcriptome is highly complex owing to numerous discontinuous transcription events. In addition to the canonical genomic and 9 subgenomic RNAs, SARS-CoV-2 produces transcripts encoding unknown ORFs with fusion, deletion, and/or frameshift. Using nanopore direct RNA sequencing, we further find at least 41 RNA modification sites on viral transcripts, with the most frequent motif, AAGAA. Modified RNAs have shorter poly(A) tails than unmodified RNAs, suggesting a link between the modification and the 3' tail. Functional investigation of the unknown transcripts and RNA modifications discovered in this study will open new directions to our understanding of the life cycle and pathogenicity of SARS-CoV-2.

INTRODUCTION

Coronavirus disease 19 (COVID-19) is caused by a novel coronavirus designated as severe acute respiratory syndrome coronavirus 2 (SARS-CoV-2) (Zhou et al., 2020; Zhu et al., 2020). Like other coronaviruses (order Nidovirales, family Coronaviridae, subfamily Coronavirinae). SARS-CoV-2 is an enveloped virus with a positive-sense, single-stranded RNA genome of $\sim\!\!30$ kb. SARS-CoV-2 belongs to the genus betacoronavirus, together with SARS-CoV and Middle East respiratory syndrome coronavirus (MERS-CoV) (with 80% and 50% homology, respectively) (Kim et al., 2020; Zhou et al., 2020). Coronaviruses (CoVs) were thought to primarily cause enzootic infections in birds and mammals. However, the recurring outbreaks of SARS, MERS. and now COVID-19 have clearly demonstrated the remarkable ability of CoVs to cross species barriers and transmit between humans (Menachery et al., 2017).

Among RNA viruses, CoVs have some of the largest genomes (26-32kb) (Figure 1). Each viral transcript has a 5'-cap structure and a 3' poly(A) tail (Lai and Stohlman, 1981; Yogo et al., 1977). Upon cell entry, the genomic RNA is translated to produce nonstructural proteins (nsps) from two open reading frames (ORFs), ORF1a and ORF1b. The ORF1a produces polypeptide 1a (pp1a, 440-500 kDa) that is cleaved into 11 nsps. The -1 ribosome frameshift occurs immediately upstream of the ORF1a stop codon, which allows continued translation of ORF1b, yielding a large polypeptide (pp1ab, 740-810 kDa) which is cleaved into 15 nsps. The proteolytic cleavage is mediated by viral proteases nsp3 and nsp5 that harbor a papain-like protease domain and a 3C-like protease domain, respectively.

The viral genome is also used as the template for replication and transcription, which is mediated by nsp12 harboring RNAdependent RNA polymerase (RdRP) activity (Snijder et al., 2016; Sola et al., 2015). Negative-sense RNA intermediates are generated to serve as the templates for the synthesis of positive-sense genomic RNA (gRNA) and subgenomic RNAs (sgRNAs). The gRNA is packaged by the structural proteins to assemble progeny virions. Shorter sgRNAs encode conserved structural proteins (spike protein [S], envelope protein [E], membrane protein [M], and nucleocapsid protein [N]), and several accessory proteins. SARS-CoV-2 is known to have at least six accessory proteins (3a, 6, 7a, 7b, 8, and 10) according to the current annotation (GenBank: NC_045512.2). However, the ORFs have not yet been experimentally verified for expression. Therefore, it is currently unclear which accessory genes are actually expressed from this compact genome.

Each coronaviral RNA contains the common 5' "leader" sequence of ~70 nt fused to the "body" sequence from the downstream part of the genome (Lai and Stohlman, 1981; Sola et al., 2015) (Figure 1). According to the prevailing model, leader-tobody fusion occurs during negative-strand synthesis at short motifs called transcription-regulatory sequences (TRSs) that are located immediately adjacent to ORFs (Figure 1), TRSs contain a conserved 6-7 nt core sequence (CS) surrounded by variable sequences. During negative-strand synthesis, RdRP pauses when it crosses a TRS in the body (TRS-B) and switches the template to the TRS in the leader (TRS-L), which results in discontinuous transcription leading to the leader-body fusion. From the fused negative-strand intermediates, positive-strand mRNAs are transcribed. The replication and transcription mechanism has been





Resource

The Arch

Dongwan Kim, 1,2 J ¹Center for RNA Resx ²School of Biological ³Korea National Instit ⁴Lead Contact *Correspondence: na

https://doi.org/10.10

SUMMARY

SARS-CoV-2 is genome was rej sequencing tech scriptome. DNA discontinuous tr CoV-2 produces pore direct RNA the most frequen a link between the modifications dipathogenicity of

INTRODUCTION

Coronavirus disease virus designated as virus 2 (SARS-CoV-

other coronaviruses (order *indovirales*, tamily *Coronavirales*, subfamily *Coronaviriales*), SARS-CoV-2 is an enveloped virus with a positive-sense, single-stranded RNA genome of ~30 kb. SARS-CoV-2 belongs to the genus *betacoronavirus*, together with SARS-CoV) with 80% and 50% homology, respectively (Kim et al., 2020; Zhou et al., 2020). Coronaviruses (CoVs) were thought to primarily cause enzootic infections in birds and mammals. However, the recurring outbreaks of SARS, MERS, and now COVID-19 have clearly demonstrated the remarkable ability of CoVs to cross species barriers and transmit between humans (Menachery et al., 2017).

Among RNA viruses, CoVs have some of the largest genomes (26-32kb) (Figure 1). Each viral transcript has a 5'-cap structure and a 3' poly(A) tail (Lai and Stohlman, 1981; Yogo et al., 1977). Upon cell entry, the genomic RNA is translated to produce nonstructural proteins (nsps) from two open reading frames (ORFs), ORF1a and ORF1b. The ORF1a produces polypeptide 1a (pp1a, 440-500 kDa) that is cleaved into 11 nsps. The -1 nibosome frameshift occurs immediately upstream of the ORF1a stop codon, which allows continued translation of ORF1b, yielding a large polypeptide (pp1ab, 740-810 kDa) which is cleaved into 15 nsps. The proteolytic cleavage is mediated by viral proteases nsp3 and nsp5 that harbor a papain-like protease domain and a 3G-like protease domain, respectively.

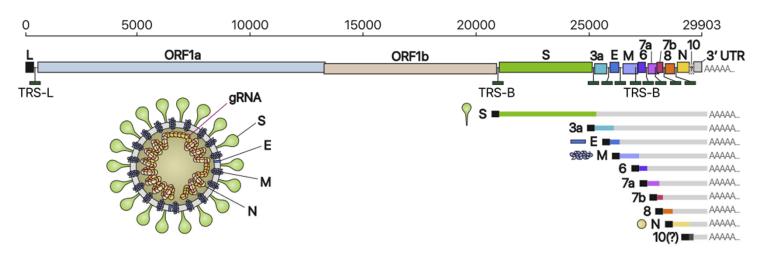


Figure 1. Schematic Presentation of the SARS-CoV-2 Genome Organization, the Canonical Subgenomic mRNAs, and the Virion Structure

From the full-length genomic RNA (29,903 nt) that also serves as an mRNA, ORF1a and ORF1b are translated. In addition to the genomic RNA, nine major subgenomic RNAs are produced. The sizes of the boxes representing small accessory proteins are bigger than the actual size of the ORF for better visualization. The black box indicates the leader sequence. Note that our data show no evidence for ORF10 expression.

postive-sense genomic HNA (giNN) and subgenomic HNAs (ggRNAs). The gRNA is packaged by the structural proteins to assemble progeny virions. Shorter sgRNAs encode conserved structural proteins (spike protein [S], envelope protein [E, membrane protein [M], and nucleocapsid protein [N]), and several accessory proteins. SARS-CoV-2 is known to have at least six accessory proteins (3a, 6, 7a, 7b, 8, and 10) according to the current annotation (GenBank: No. Q455122.) However, the ORFs have not yet been experimentally verified for expression. Therefore, it is currently unclear which accessory genes are actually expressed from this compact genome.

Each coronaviral RNA contains the common 5' "leader" sequence of ~70 nt fused to the "body" sequence from the downstream part of the genome (Lai and Stohlman, 1981; Sola et al., 2015) (Figure 1). According to the prevailing model, leader-to-body fusion occurs during negative-strand synthesis at short motifs called transcription-regulatory sequences (TRSs) that are located immediately adjacent to ORFs (Figure 1). TRSs contain a conserved 6-7 nt core sequence (CS) surrounded by variable sequences. During negative-strand synthesis, RdRP pauses when it crosses a TRS in the body (TRS-B) and switches the template to the TRS in the leader (TRS-L), which results in discontinuous transcription leading to the leader-body fusion. From the fused negative-strand intermediates, positive-strand mRNAs are transcribed. The replication and transcription mechanism has been

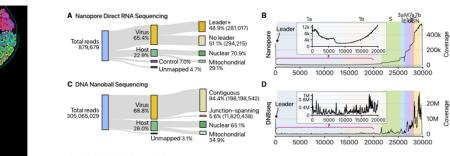


Figure 2. Statistics of Sequencing Data

(A) Read counts from nanopore direct RNA sequencing of total RNA from Vero cells infected with SARS-CoV-2. "Leader+" indicates the viral reads that contain the 5° end leader sequence. "No leader" denotes the viral reads lacking the leader sequence. "Nuclear" reads match mRNAs from the nuclear chromosome while "mitochondrial" reads are derived from the mitochondrial genome. "Control" indicates quality control RNA for nanopore sequencing.
(B) Genome coverage of the nanopore direct RNA sequencing data shown in (N). The stepwise reduction in coverage corresponds to the borders expected for the

canonical sgRNAs. The smaller inner plot magnifies the 5′ part of the genome.

(C) Read counts from DNA nanoball sequencing using MGISEQ. Total RNA from Vero cells infected with SARS-CoV-2 was used for sequencing.

(D) Genome coverage of the DNA nanoball sequencing (DNB-seq) data shown in (C).

(Punh for special

Resource

The Architecture of SARS-CoV-2 Transcriptome

Dongwan Kim, 1.2 Joo-Yeon Lee, 3 Jeong-Sun Yang, 3 Jun Won Kim, 3 V. Narry Kim, 1.2.4.* and Hyeshik Chang 1.2.*

The v

and trai

depend

2016: \$

positive

(sgRNA

assemb

structu

the ORI

sion. Th

are act

Each

¹Center for RNA Research, Institute for Basic Science (IBS), Seoul 08826, Repu 2School of Biological Sciences, Seoul National University, Seoul 08826, Republ ³Korea National Institute of Health, Korea Centers for Disease Control and Prev

*Correspondence: narrykim@snu.ac.kr (V.N.K.), hyeshik@snu.ac.kr (H.C.) https://doi.org/10.1016/j.cell.2020.04.011

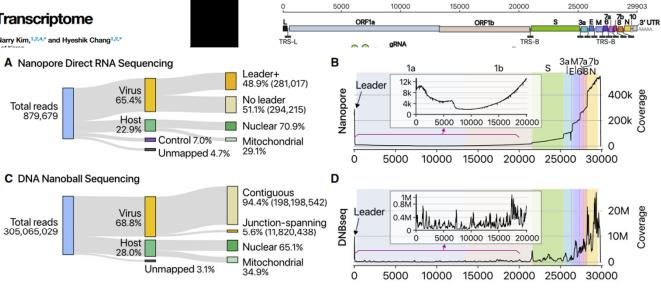
SUMMARY

SARS-CoV-2 is a betacoronavirus responsible for the CO\ genome was reported recently, its transcriptomic architectu sequencing techniques, we present a high-resolution map of scriptome. DNA nanoball sequencing shows that the transcr discontinuous transcription events. In addition to the canoni CoV-2 produces transcripts encoding unknown ORFs with fu pore direct RNA sequencing, we further find at least 41 RN the most frequent motif, AAGAA. Modified RNAs have shorter a link between the modification and the 3' tail. Functional inve modifications discovered in this study will open new direction pathogenicity of SARS-CoV-2.

INTRODUCTION

Coronavirus disease 19 (COVID-19) is caused by a novel coronavirus designated as severe acute respiratory syndrome coronavirus 2 (SARS-CoV-2) (Zhou et al., 2020; Zhu et al., 2020), Like other coronaviruses (order Nidovirales, family Coronaviridae, subfamily Coronavirinae). SARS-CoV-2 is an enveloped virus with a positive-sense, single-stranded RNA genome of ~30 kb. SARS-CoV-2 belongs to the genus betacoronavirus, together with SARS-CoV and Middle East respiratory syndrome coronavirus (MERS-CoV) (with 80% and 50% homology, respectively) (Kim et al., 2020; Zhou et al., 2020). Coronaviruses (CoVs) were thought to primarily cause enzootic infections in birds and to the mammals. However, the recurring outbreaks of SARS, MERS. and now COVID-19 have clearly demonstrated the remarkable ability of CoVs to cross species barriers and transmit between humans (Menachery et al., 2017).

Among RNA viruses, CoVs have some of the largest genomes (26-32kb) (Figure 1). Each viral transcript has a 5'-cap structure and a 3' poly(A) tail (Lai and Stohlman, 1981; Yogo et al., 1977). Upon cell entry, the genomic RNA is translated to produce nonstructural proteins (nsps) from two open reading frames (ORFs), ORF1a and ORF1b. The ORF1a produces polypeptide 1a (pp1a. 440-500 kDa) that is cleaved into 11 nsps. The -1 ribosome frameshift occurs immediately upstream of the ORF1a stop codon, which allows continued translation of ORF1b, yielding a large polypeptide (pp1ab, 740-810 kDa) which is cleaved into 15 nsps. The proteolytic cleavage is mediated by viral proteases nsp3 and nsp5 that harbor a papain-like protease domain and a 3C-like protease domain, respectively.



Cell

Resource

Figure 2. Statistics of Sequencing Data

(A) Read counts from nanopore direct RNA sequencing of total RNA from Vero cells infected with SARS-CoV-2. "Leader+" indicates the viral reads that contain the 5' end leader sequence. "No leader" denotes the viral reads lacking the leader sequence. "Nuclear" reads match mRNAs from the nuclear chromosome while "mitochondrial" reads are derived from the mitochondrial genome. "Control" indicates quality control RNA for nanopore sequencing.

- (B) Genome coverage of the nanopore direct RNA sequencing data shown in (A). The stepwise reduction in coverage corresponds to the borders expected for the canonical sgRNAs. The smaller inner plot magnifies the 5' part of the genome.
- (C) Read counts from DNA nanoball sequencing using MGISEQ. Total RNA from Vero cells infected with SARS-CoV-2 was used for sequencing.
- (D) Genome coverage of the DNA nanoball sequencing (DNB-seq) data shown in (C).

See also Figure S1. body fu

tifs called transcription-regulatory sequences (TRSs) that are located immediately adjacent to ORFs (Figure 1), TRSs contain a conserved 6-7 nt core sequence (CS) surrounded by variable seguences. During negative-strand synthesis, RdRP pauses when it crosses a TRS in the body (TRS-B) and switches the template to the TRS in the leader (TRS-L), which results in discontinuous transcription leading to the leader-body fusion. From the fused negative-strand intermediates, positive-strand mRNAs are transcribed. The replication and transcription mechanism has been Unmapped 3.1% 10000 15000 20000 25000 30000

Figure 2. Statistics of Sequencing Data

(A) Read counts from nanopore direct RNA sequencing of total RNA from Vero cells infected with SARS-CoV-2. "Leader+" indicates the viral reads that contain the 5' end leader sequence, "No leader" denotes the viral reads lacking the leader sequence, "Nuclear" reads match mRNAs from the nuclear chromosome while "mitochondrial" reads are derived from the mitochondrial genome. "Control" indicates quality control RNA for nanopore sequencing (B) Genome coverage of the nanopore direct RNA sequencing data shown in (A). The stepwise reduction in coverage corresponds to the bo

canonical sgRNAs. The smaller inner plot magnifies the 5' part of the geno (C) Read counts from DNA nanoball sequencing using MGISEQ. Total RNA from Vero cells infected with SARS-CoV-2 was used for sequencing. (D) Genome coverage of the DNA nanoball sequencing (DNB-seq) data shown in (C).



sequence the terminal \sim 12 nt (Figure 2B). The longest tags (111 reads) correspond to the full-length gRNA (Figure 2B). The coverage of the 3' side of the viral genome is substantially higher than that of the 5' side, which reflects the nested sgRNAs. This is also partly due to the 3' bias of the directional DRS

technique. The nt) in viral RNA end, as expect in the coverag body junction i DRS reads, wit

> a link between the modifi modifications discovered pathogenicity of SARS-C

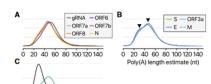
INTRODUCTION

Coronavirus disease 19 (COVIÍ virus designated as severe act virus 2 (SARS-CoV-2) (Zhou e other coronaviruses (order A subfamily Coronaviruses), SAI with a positive-sense, single-SARS-CoV-2 belongs to the with SARS-CoV and Middle Ea rus (MERS-CoV) (with 80% a Cign et al., 22 thought to primarily cause € mammals. However, the recu

ability of CoVs to cross species parners and transmit between humans (Menachery et al., 2017).

Among RNA viruses, CoVs have some of the largest genomes (26-32kb) (Figure 1). Each viral transcript has a 5'-cap structure and a 3' poly(A) tail (Lai and Stohlman, 1981; Yogo et al., 1977). Upon cell entry, the genomic RNA is translated to produce nonstructural proteins (nsps) from two open reading frames (ORFs), ORF1a and ORF1b. The ORF1a produces polypeptide 1a (pp1a, 440-500 kDa) that is cleaved into 11 nsps. The -1 ribosome frameshift occurs immediately upstream of the ORF1a stop codon, which allows continued translation of ORF1b, yielding a large polypeptide (pp1ab, 740-810 kDa) which is cleaved into 15 nsps. The proteolytic cleavage is mediated by viral proteases nsp3 and nsp5 that harbor a papain-like protease domain and a 3C-like protease domain, respectively.

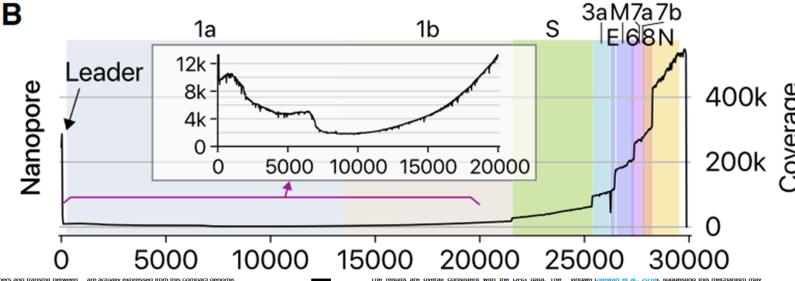
Cell Resource



CellPress

sgRNAs (Figure 3B). Quantitative comparison of the junctionspanning reads shows that the N RNA is the most abundantly expressed transcript, followed by S, 7a, 3a, 8, M, E, 6, and 7b (Figure 3C).

It is important to note that ORF10 is represented by only one read in DNB data (0.000009% of viral junction-spanning reads) and that it was not supported at all by DRS data. ORF10 does not show significant homology to known proteins. Thus, ORF10 is unlikely to be expressed. The annotation of ORF10



are actually expressed from this compact genome.

Each coronaviral RNA contains the common 5' "leader

each coronaval RNA contains the common 5 "leader" sequence for Mr 2011 tiles of to the "body" sequence from the downstream part of the genome (Lai and Stohlman, 1981; Sola et al., 2015) ("igure 1). According to the prevailing model, leader-body fusion occurs during negative-strand synthesis at short motifs called transcription-regulatory sequences ((TRSs) that are located immediately adjacent to ORFs (Figure 1). TRSs contain a conserved 6-7 nt core sequence (CS) surrounded by variable sequences. During negative-strand synthesis, RdRP pauses when it crosses a TRS in the body (TRS-B) and switches the template to the TRS in the leader (TRS-L), which results in discontinuous transcription leading to the leader-body fusion. From the fused negative-strand intermediates, positive-strand mRNAs are transcribed. The replication and transcription mechanism has been

leader-body junctions are frequently sequenced, giving rise to a sharp peak at the 5' end in the coverage plot (Figure 2D). The 3' end exhibits a high coverage as expected for the nested transcripts.

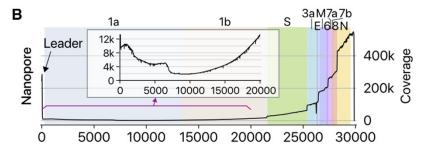
The depth of DNB-seq allowed us to confirm and examine the junctions on an unprecedented scale for a CoV genome. We mapped the 5' and 3' breakpoints at the junctions and estimated the fusion frequency by counting the reads spanning the junctions (Figure 3A). The leader represents the most prominent 5' site, as expected (Figure 3A, red asterisk on the x axis). The known TRS-Bs are detected as the top 3' sites (Figure 3A, red dots on the y axis). These results confirm that SARS-CoV-2 uses the canonical TRS-mediated template-switching mechanism for discontinuous transcription to produce major

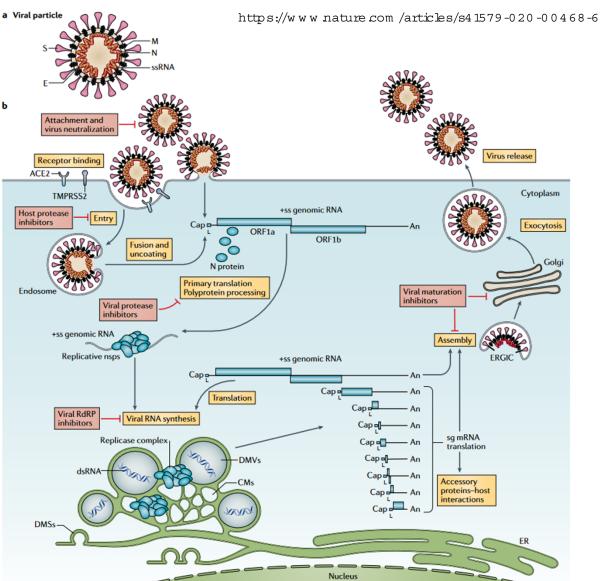
vincaer (Stewart et al., 201e), suggesting this mechanism may be at least partially conserved in coronaviridae. Functionality of sgRNAs are not clear, and some of them have been considered as parasites that compete for viral proteins, hence referred to a defective interfering RNAs; 01-RNAs; (Pathak and Nary, 2009).

Although the noncanonical transcripts may arise from erroneous replicase activity, it remains an open question if the fusion has an active role in viral life cycle and evolution. Although individual RNA species are not abundant, the combined read numbers are often comparable to the levels of accessory transcripts. Most of the RNAs have coding potential to yield proteins. Transcripts that belong to the "TRS-L-independent distant" group encode the upstream part of ORF1a, including nsp1, truncated nsp2, and/or truncated nsp3, whose summed abundance is ~20% of gRNA. Depending on translation efficiency.

(Posts for specification







Viehweger et al.

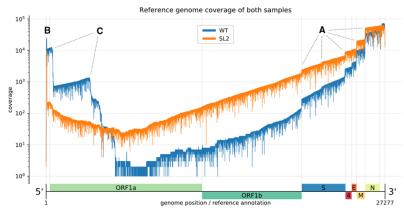


Figure 2. Reference genome coverage of the HCoV-229E WT sample (blue) and the SL2 sample (orange) based on alignments with minimap2. There is an inverse correlation between sq RNA abundance and length. (A) Notable vertical "steps" in the coverage correspond to borders expected for the canonical sg RNAs (see Fig. 1). (B) The presence of the leader sequence (~65 nt) in canonical sg RNAs gives rise to the sharp coverage peak at the 5'-end. (C) We also observed unexpected "steps," especially in the WT sample (blue). We hypothesize that the sequences correspond to DI-RNA molecules that may arise by recombination at TRS-like sequence motifs as well as other sites displaying sequence similarities that are sufficient to support illegitimate recombination events (see Fig. 3). We attribute the difference in the observed (noncanonical) recombination sites between the two samples to biological factors that we either did not control for or do not know (see also legend to Fig. 3).



Method-

Direct RNA nanopore sequencing of full-length coronavirus genomes provides novel insights into structural variants and enables modification analysis

Adrian Viehweger, 1,2,5 Sebastian Krautwurst, 1,2,5 Kevin Lamkiewicz, 1,2 Ramakanth Madhugiri,³ John Ziebuhr,^{2,3} Martin Hölzer,^{1,2} and Manja Marz^{1,2,4}

¹RNA Bioinformatics and High-Throughput Analysis, Friedrich Schiller University Jena, 07743 Jena, Germany; ²European Virus Bioinformatics Center, Friedrich Schiller University Jena, 07743 Jena, Germany; ³Institute of Medical Virology, Justus Liebiq University Gießen, 35390 Gießen, Germany; ⁴Leibniz Institute on Aging-Fritz Lipmann Institute, 07743 Jena, Germany

Sequence analyses of RNA virus genomes remain challenging owing to the exceptional genetic plasticity of these viruses. Because of high mutation and recombination rates, genome replication by viral RNA-dependent RNA polymerases leads to populations of closely related viruses, so-called "quasispecies." Standard (short-read) sequencing technologies are ill-suited to reconstruct large numbers of full-length haplotypes of (I) RNA virus genomes and (2) subgenome-length (sg) RNAs composed of noncontiguous genome regions. Here, we used a full-length, direct RNA sequencing (DRS) approach based on nanopores to characterize viral RNAs produced in cells infected with a human coronavirus. By using DRS, we were able to map the longest (~26-kb) contiguous read to the viral reference genome. By combining Illumina and Oxford Nanopore sequencing, we reconstructed a highly accurate consensus sequence of the human coronavirus (HCoV)-229E genome (27.3 kb). Furthermore, by using long reads that did not require an assembly step, we were able to identify, in infected cells, diverse and novel HCoV-229E sg RNAs that remain to be characterized. Also, the DRS approach, which circumvents reverse transcription and amplification of RNA, allowed us to detect methylation sites in viral RNAs. Our work paves the way for haplotype-based analyses of viral quasispecies by showing the feasibility of intra-sample haplotype separation. Even though several technical challenges remain to be addressed to exploit the potential of the nanopore technology fully, our work illustrates that DRS may significantly advance genomic studies of complex virus populations, including predictions on long-range interactions in individual full-length viral RNA haplotypes.

(Supplemental material is available for this article.)

Coronaviruses (subfamily Coronavirinae, family Coronaviridae, order Nidovirales) are enveloped positive-sense (+) single-stranded (ss) RNA viruses that infect a variety of mammalian and avian hosts and are of significant medical and economic importance, as illustrated by recent zoonotic transmissions from diverse animal hosts to humans (Vijay and Perlman 2016; Menachery et al. 2017). The genome sizes of coronaviruses (~30 kb) exceed those of most other RNA viruses. Coronaviruses use a special mechanism called discontinuous extension of minus strands (Sawicki and Sawicki 1995. 1998) to produce a nested set of 5'- and 3'-coterminal subgenomic (sg) mRNAs that carry a common 5' leader sequence that is identical to the 5'-end of the viral genome (Zuniga et al. 2004; Sawicki et al. 2007). These sg mRNAs contain a different number of open reading frames (ORFs) that encode the viral structural proteins and several accessory proteins. With very few exceptions, only the 5'-located ORF (which is absent from the next smaller sg mRNA) is translated into protein (Fig. 1).

In HCoV-229E-infected cells, a total of seven major viral RNAs are produced. The viral genome is also referred to as mRNA 1 because it has an mRNA function. In its 5'-terminal region, the genome RNA contains two large ORFs, 1a and 1b, that encode the viral replicase polyproteins 1a and 1ab. mRNAs 2, 4, 5, 6,

⁵These authors contributed equally to this work. Corresponding author: manja@uni-jena.de Article published online before print. Article, supplement

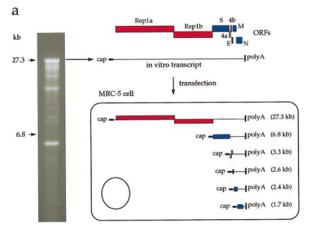
nome.org/cgi/doi/10.1101/gr.247064.118.

and 7 are used to produce the S protein, accessory protein 4, E protein, M protein, and N protein, respectively. The 5'-region of mRNA 3 contains a truncated fragment of ORF S, which is considered defective. Although this sg RNA has been consistently identified in HCoV-229E-infected cells, its mRNA function has been disputed, and there is currently no evidence that this RNA is translated into protein (Schreiber et al. 1989; Raabe et al. 1990; Thiel et al. 2003).

Like many other +RNA viruses, coronaviruses show high rates of recombination (Lai 1992; Liao and Lai 1992; Furuya et al. 1993). In fact, the mechanism to produce 5' leader-containing sg mRNAs represents a prime example for copy-choice RNA recombination that, in this particular case, is guided by complex RNA-RNA interactions involving the transcription-regulating sequence (TRS) core sequences and likely requires additional interactions of viral proteins with specific RNA signals. In other virus systems, RNA recombination has been shown to generate "transcriptional units" that control the expression of individual components of the genome (Holmes 2009). The mechanisms involved in viral RNA recombination are diverse and may even extend to nonreplicating systems (Gallei et al. 2004). In the vast majority of cases, recombination

© 2019 Viehweger et al. This article is distributed exclusively by Cold Spring Harbor Laboratory Press for the first six months after the full-issue publication date (see http://genome.cshlp.org/site/misc/terms.xhtml). After six months, it is available under a Creative Commons License (Attribution-NonCommercial 4.0 International), as described at http://creativecommons.org/licenses/by





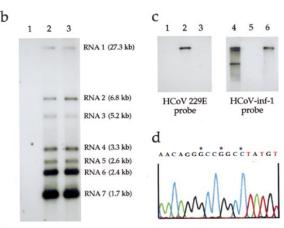


Fig. 3. Recovery of recombinant human coronavirus. (a) Ethidium bromide-stained, 1% agarose gel in which 1 µg capped RNA, transcribed in vitro from wHCoV-in-1 DNA, has been electrophoresed. The full-length (27-3 kb) in vitro transcription product is indicated. Also shown is the structural relationship of the HCoV ORFs, the in vitro-transcribed HCoV-in-f1-1 RNA and the predicted genomic and subgenomic mRNAs in HCoV-in-f1-1 RNA-transfected MRC-5 cells. (b) Analysis of poly(A)-containing RNA from parental virus-and recombinant virus-infected cells. Poly(A)-containing RNA from parental virus-and recombinant wirus-infected cells. Poly(A)-containing RNA was isolated from MRC-5 cells that had been mock-infected (lane 1), infected with parental HCoV 229E virus (lane 2) or infected with recombinant HCoV-in-f1-1 virus (lane 3). The RNA was analysed by Northern hybridization using a ³²P-end-labelled oligonucleotide (5' AGAWACTTCATCACG-CACTGG 3') corresponding to nt 26802–26822 within the HCoV uncleocapsid protein gene. The characteristic set of genomic and subgenomic HCoV mRNAs is indicated. (c) Northern hybridization of in viro-transcribed HCoV-in-f1-1 RNA (lanes 1 and 4) and poly(A)-containing RNA from parental HCoV 229E-infected MRC-5 cells (lanes 2 and 5) and HCoV-in-f1-1 infected MRC-5 cells (lanes 3 and 6). The RNAs were probed with a parental HCoV 229E-specific oligonucleotide, 5' ACATACGCTGGGCCTGTT 3' (lanes 1-3), or an HCoV-in-f1-specific oligonucleotide, 5' ACATACGCTGGGCCCTGTT 3' (lanes 1-3), or an HCoV-in-f1-specific oligonucleotide, 5' ACATACGCTGGGCCTGTT 3' (lanes 1-3), or an HCoV-in-f1-specific oligonucleotide, 5' ACATACGCTGGGCCTGTT 3' (lanes 1-3), or an HCoV-in-f1-specific oligonucleotide, 5' ACATACGCTGGGCCCTGTT 3' (lanes 1-3), or an HCoV-in-f1-specific oligonucleotide mutations specific to the recombinant virus genome. The three nucleotide mutations are indicated that represent the diagnostic Feel size

Infectious RNA transcribed in vitro from a cDNA copy of the human coronavirus genome cloned in vaccinia virus

Volker Thiel, Jens Herold,† Barbara Schelle and Stuart G. Siddell

Institute of Virology and Immunology, University of Würzburg, Versbacher Straße 7, 97078 Würzburg, Germany

The coronavirus genome is a positive-strand RNA of extraordinary size and complexity. It is composed of approximately 30000 nucleotides and it is the largest known autonomously replicating RNA. It is also remarkable in that more than two-thirds of the genome is devoted to encoding proteins involved in the replication and transcription of viral RNA. Here, a reverse-genetic system is described for the generation of recombinant coronaviruses. This system is based upon the *in vitro* transcription of infectious RNA from a cDNA copy of the human coronavirus 229E genome that has been cloned and propagated in vaccinia virus. This system is expected to provide new insights into the molecular biology and pathogenesis of coronaviruses and to serve as a paradigm for the genetic analysis of large RNA virus genomes. It also provides a starting point for the development of a new class of eukaryotic, multi-gene RNA vectors that are able to express several proteins simultaneously.

Introduction

Coronaviruses are enveloped, vertebrate viruses that are associated mainly with respiratory and enteric diseases. The human coronaviruses are responsible for 10-20% of all common colds (McIntosh, 1996). The virus genome is a positive-strand RNA of approximately 30 kb that encodes a minimal set of four structural proteins and a large array of nonstructural proteins involved in replication and transcription (Lai & Cavanagh, 1997; Siddell & Snijder, 1998). These socalled replicase proteins are encoded in two overlapping open reading frames (ORFs) that extend about 20 kb from the 5' end of the genome. It is a hallmark of coronaviruses that extensive co- and post-translational proteolytic processing is required to produce the proteins needed to assemble a functional replication-transcription complex (Ziebuhr et al., 2000). It is also noteworthy that the generation of coronavirus subgenomic mRNAs involves an unusual process of discontinuous transcription (Spaan et al., 1983), most probably during the

Author for correspondence: Stuart Siddell.

Fax +49 931 201 3970. e-mail siddell@vim.uni-wuerzburg.de

† **Present address**: SWITCH-Biotech AG, Fraunhofer Straße 10, 82152 Martinsried, Germany.

The GenBank accession number of the sequence reported in this paper is AF304460.

synthesis of subgenomic, negative-strand templates (Sawicki & Sawicki, 1998). Discontinuous transcription is a highly regulated process and is, at least in part, dependent upon basepairing between cis-acting elements, the so-called transcription-associated sequences, located at the 5' end of the genome and at various 3'-proximal sites (van Marle et al., 1999).

Until recently, the study of coronavirus genetics was essentially restricted to the analysis of temperature-sensitive (ts) mutants (Lai & Cavanagh, 1997; Stalcup et al., 1998), the analysis of defective RNA templates that depend upon replicase proteins provided by a helper virus (Repass & Makino, 1998; Izeta et al., 1999; Williams et al., 1999) and the analysis of chimeric viruses generated by targetted recombination (Fischer et al., 1997; Hsue & Masters, 1999; Kuo et al., 2000). This was because the large size of the coronavirus genome and the instability of some coronavirus cDNAs in bacteria effectively precluded the use of cloning procedures that have been used to generate infectious RNA from cDNA copies of other positive-strand RNA virus genomes (Ruggli & Rice, 1999). Recently, however, two different approaches have been developed that appear to overcome these problems. Firstly, Almazán et al. (2000) have reported that the cloning of full-length, transmissible gastroenteritis virus (TGEV) cDNA in a bacterial artificial chromosome, combined with nuclear expression of infectious RNA, can be used to produce recombinant virus. Secondly, Yount et al. (2000) have described a system to assemble a full-length cDNA construct of the

0001-7678 © 2001 SGM

Replication and Packaging of Coronavirus Infectious Bronchitis Virus Defective RNAs Lacking a Long Open Reading Frame

ZOLTÁN PÉNZES,1† CHRISTINE WROE,2 T. DAVID K. BROWN,2 PAUL BRITTON,18 AND DAVID CAVANAGH1

Division of Molecular Biology, Institute for Animal Health, Compton Laboratory, Compton, and Division of Virology, Department of Pathology, University of Cambridge, Cambridge, 2 United Kingdom

Received 19 June 1996/Accepted 9 September 1996

The construction of a full-length clone of the avian coronavirus infectious bronchitis virus (IBV) defective RNA (D-RNA), CD-91 (9,080 nucleotides [Z. Penzes et al., Virology 203:286-293]), downstream of the bacteriophage T7 promoter is described. Electroporation of in vitro T7-transcribed CD-91 RNA into IBV helper virus-infected primary chick kidney cells resulted in the production of CD-91 RNA as a replicating D-RNA in subsequent passages. Three CD-91 deletion mutants were constructed-CD-44, CD-58, and CD-61-in which 4,639, 3,236, and 2,953 nucleotides, respectively, were removed from CD-91, resulting in the truncation of the CD-91 long open reading frame (ORF) from 6,465 to 1,311, 1,263, or 2,997 nucleotides in CD-44, CD-58, or CD-61, respectively. Electroporation of in vitro T7-transcribed RNA from the three constructs into IBV helper virus-infected cells resulted in the replication and packaging of CD-58 and CD-61 but not CD-44 RNA. The ORF of CD-61 was further truncated by the insertion of stop codons into the CD-61 sequence by PCR mutagenesis, resulting in constructs CD-61T11 (ORF: nucleotides 996 to 1,058, encoding 20 amino acids), CD-61T22 (ORF: nucleotides 996 to 2,294, encoding 432 amino acids), and CD-61T24 (ORF: nucleotides 996 to 2,450, encoding 484 amino acids), all of which were replicated and packaged to the same levels as observed for either CD-61 or CD-91. Analysis of the D-RNAs showed that the CD-91- or CD-61-specific long OREs had not been restored. Our data indicate that IBV D-RNAs based on the natural D-RNA, CD-91, do not require a long ORF for efficient replication. In addition, a 1.4-kb sequence, corresponding to IBV sequence at the 5' end of the 1b gene, may be involved in the packaging of IBV D-RNAs or form part of a cis-acting replication element.

Infectious bronchitis virus (IBV), a member of the Coronavirus genus of the Coronaviridae family, is an enveloped virus with a single-stranded, positive-sense RNA genome of 27,608 nucleotides (1) that is 5' capped and 3' polyadenylated. A 3'-coterminal nested set of six subgenomic mRNAs are synthesized in IBV-infected cells which possess a 63-nucleotide leader sequence at their 5' ends which is also located at the 5' end of the genomic RNA.

Following high-multiplicity passage of RNA viruses, defective RNAs (D-RNAs) may be produced which lack internal parts of the genome, require helper virus for their replication, and may interfere with the replication of the helper virus (6). For coronaviruses D-RNAs have been produced from mouse hepatitis virus (MHV) (17, 25), bovine coronavirus (BCV) (2), IBV (22), and transmissible gastroenteritis virus (20). A characteristic of all naturally occurring coronavirus D-RNAs is the presence of a long open reading frame (ORF), corresponding to ≥70% of the RNA, and usually comprising in-frame fusions between different discontinuous regions of the polymerase gene and varying amounts of the nucleocapsid protein (N) gene (2, 16, 18, 22, 25). Although D-RNA-specific proteins have been detected in MHV D-RNA-replicating cells (4, 8, 16, 18), the requirement for a D-RNA-specific ORF is unclear. Differences in the MHV D-RNA-specific ORF products tend

to rule out a specific cis-acting role for them. However, the product of the N-protein sequence present in the 2.2-kb BCV D-RNA has been demonstrated to have a requirement in cis for optimum replication (3).

The study of coronavirus D-RNAs has involved mainly the characterization of three MHV-derived D-RNAs: the 5.5-kb MHV A59 D-RNA, DI-a (4), and two D-RNAs derived from MHV JHM, the 3.4-kb DIssE and the 2.2-kb DIssE (14). Although each MHV D-RNA contains a long ORF, expressed in D-RNA-infected cells, their sequences are substantially different. Truncation of the ORF in DI-a did not prevent replication but did result in a reduced accumulation of the altered D-RNA (4). The replication of a series of mutant DI-a-derived RNAs with in-frame and out-of-frame ORFs showed that those with in-frame ORFs prevailed within three passages compared to their out-of-frame counterparts, indicating that the ORF is required for efficient propagation. This result was supported by the observation that passage of D-RNAs with out-of-frame ORFs resulted in the emergence of RNAs with restored ORFs, indicating that the presence of an ORF had some selective advantage (4). Recent work has demonstrated that it is not the particular encoded sequence but translation of an ORF per se that is required for replication (26). The conclusion that a long ORF in MHV D-RNAs is required for efficient propagation was supported by the observation that replication of a 2.2-kb BCV D-RNA was inhibited following the introduction of frameshift mutations for truncation of the long ORF (2). In contrast, the long ORFs of the MHV JHM D-RNAs DISSE (7) and DIssF (13) did not appear to be required for replication following deletion mutagenesis to study the role of cis-acting sequences in replication. However, a derivative of DIssE, NE-1, containing a single nucleotide deletion resulting in truncation of the ORF product from 567 to 57 amino acids, was

* Corresponding author.

JOURNAL OF VIROLOGY, May 1985, p. 329-336 0022-538X/85/050329-08\$02.00/0 Copyright © 1985, American Society for Microbiology

Structure of the Intracellular Defective Viral RNAs of Defective Interfering Particles of Mouse Hepatitis Virus

SHINJI MAKINO,†* NOBORU FUJIOKA, AND KOSAKU FUJIWARA

Department of Animal Pathology, Institute of Medical Science, University of Tokyo, 4-6-1, Shirokanedai, Minato-ku, Tokyo 108, Japan

Received 6 September 1984/Accepted 22 January 1985

The intracellular defective RNAs generated during high-multiplicity serial passages of mouse hepatitis virus JHM strain on DBT cells were examined. Seven novel species of single-stranded polyadenylic acid-containing defective RNAs were identified from passages 3 through 22. The largest of these RNAs, DIssA (molecular weight [mw], 5.2×10^6), is identical to the genomic RNA packaged in the defective interfering particles produced from these cells. Other RNA species, DIssB1 (mw, 1.9×10^6 to 1.6×10^6), DIssB2 (mw, 1.6×10^6), DISSC (mw, 2.8×10^6) DISSD (mw, 0.82×10^6), DISSE (mw, 0.78×10^6), and DISSF (mw, 1.3×10^6) were detected at different passage levels. RNase T1-resistant oligonucleotide fingerprinting demonstrated that all these RNAs were related and had multiple deletions of the genomic sequences. They contained different subsets of the genomic sequences from those of the standard intracellular mRNAs of nondefective mouse hepatitis virus JHM strain. Thus these novel intracellular viral RNAs were identified as defective interfering RNAs of mouse hepatitis virus JHM strain. The synthesis of six of the seven normal mRNA species specific to mouse hepatitis virus JHM strain was completely inhibited when cells were infected with viruses of late-passage levels. However, the synthesis of RNA7 and its product, viral nucleoprotein, was not significantly altered in late passages. The possible mechanism for the generation of defective interfering RNAs was discussed.

Over the last few years many of the steps in the replication of coronaviruses, particularly mouse hepatitis virus (MHV) and infectious bronchitis virus, have been elucidated (30, 31). The genomic RNA of MHV encodes RNA-dependent RNA polymerases (2, 3, 17), which are responsible for the synthesis of a genome-sized negative-stranded RNA (12). The negative-sensed RNA then serves as the template for the synthesis of both six species of subgenomic mRNAs and a genome-sized RNA (1, 12). These mRNAs are arranged in the form of a 3' coterminal "nested set." In addition, each mRNA has a common leader sequence at its 5' terminus which is derived from the 5' end of the genome (1, 9, 11, 34). Translation of different viral polypeptides is initiated independently (26, 27). Several studies have shown that mRNA7. mRNA6, and mRNA3 encode the virion nucleocapsid protein (NP), the matrix protein (E1), and the precursor of peplomer protein (E2), respectively (16, 25, 27, 29).

Defective interfering (DI) particles are deletion mutants which cannot replicate by themselves but interfere specifically with replication of the homologous virus, which is in turn required for the generation and replication of the DI particles. Many studies have focused on the role of DI virus genomes in virus evolution and in persistent infection. Although coronaviruses tend to establish persistent infection in tissue culture (30), in contrast to other positive-stranded viruses, there have been no reports about the isolation of coronavirus DI particles during persistent infection. The generation of coronavirus DI particles during high-multiplicity passages of the JHM strain of MHV (MHV-JHM) was recently reported (18). These DI particles differ from standard virus in that they contain a single positive-stranded RNA (molecular weight [mw], 5.2 × 10⁶) which is smaller than the genomic RNA of the standard virus (mw, 5.4×10^6).

Oligonucleotide fingerprinting studies indicated that the RNA of MHV-JHM DI particles had lost several large RNase T₁-resistant oligonucleotides. In the experiments in this study, we further examined the RNA synthesis in the DI-infected cells. We identified seven novel polyadenylic acid-containing intracellular DI-specific RNAs, which were generated at different times during undiluted passage of the virus. Using oligonucleotide fingerprinting, we have shown that these DI RNAs contain multiple deletions. Furthermore, the synthesis of six of the seven MHV-JHM-specific genomic and subgenomic RNAs was inhibited after infection with late-passage viruses. Interestingly, the synthesis of RNA7 and its product NP was not inhibited. The possible mechanism for the synthesis of these DI RNAs is discussed.

MATERIALS AND METHODS

Virus and cell culture. The standard MHV-JHM and serially passaged viruses were grown on DBT cells (mouse cell line transformed by the Schmidt-Ruppin strain of Rous sarcoma virus) (7) as described previously (18).

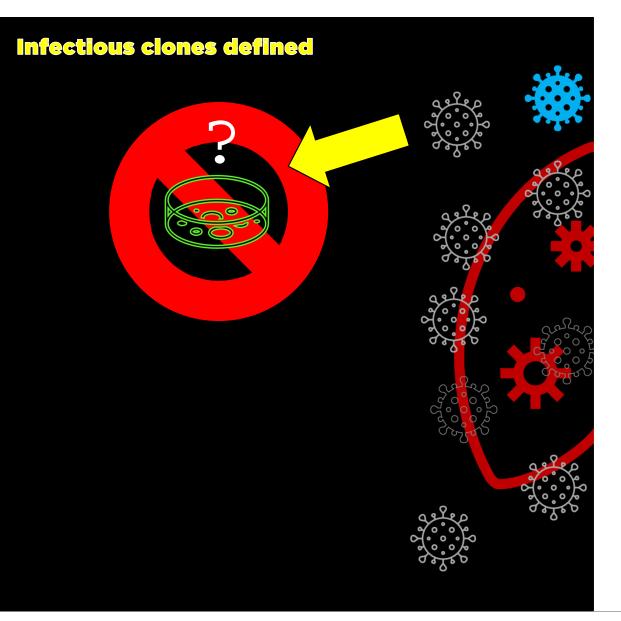
Preparation of intracellular viral RNA. 32P-labeled intracellular viral RNA was extracted by procedures described previously (21). Briefly, a monolayer culture of DBT cells was infected with viruses at a multiplicity of infection of 1.0 and labeled with ³²P_i from 6 to 9 h postinfection in the presence of 2.5 µg of actinomycin D per ml. Cytoplasmic extracts were prepared by lysing the cells in NTE buffer (0.1 M NaCl, 0.01 M Tris-hydrochloride [pH 7.2], 1 mM EDTA) containing 0.5% Nonidet P-40. RNA was isolated by phenolchloroform extractions as described previously (18).

Agarose gel electrophoresis. Analytical gel electrophoresis was conducted after denaturation of RNA with glyoxal treatment as described previously (22). Preparative gel electrophoresis in 1% urea-agarose gel was performed by published procedures (18). Each RNA species was purified by two cycles of urea-agarose gel electrophoresis to avoid contamination of smaller-sized RNAs. The RNA was eluted

^{*} Corresponding author. Mailing address: Division of Molecular Biology, Institute for Animal Health, Compton Laboratory, Compton, Newbury, Berkshire RG20 7NN, United Kingdom. Phone: (44) 1635 578411. Fax: (44) 1635 577263. Electronic mail address: Paul Britton

[†] Present address: Centro Nacional de Biotechnología, Consejo Superior de Investigaciones Científicas, Campus Universidad Autónoma, Cantoblanco, 28049 Madrid, Spain.

[†] Present address: Department of Microbiology, School of Medicine, University of Southern California, Los Angeles, CA 90033.





RESEARCH ARTICLE



Generation and Functional Analysis of Defective Viral Genomes during SARS-CoV-2 Infection

Terry Zhou,* Nora J. Gilliam,**Mc Sizhen Li,** Simone Spandau,* Raven M. Osborn,** Sarah Connor,** © Christopher S. Anderson,*
Thomas J. Mariani,** Juilee Thakar,**** Stephen Dewhurst,* David H. Mathews,** Liang Huang,** © Yan Sun**

*Department of Immunology and Microbiology, University of Rochester Medical Center, Rochester, New York, USA

Medical Scientist Training Program, University of Rochester School of Medicine and Dentistry, Rochester, New York, USA

Translational Biomedical Sciences PhD Program, University of Rochester School of Medicine and Dentistry, Rochester, New York, USA

School of Electrical Engineering & Computer Science, Oregon State University, Corvallis, Oregon, USA

"Department of Pediatrics and Center for Children's Health Research, University of Rochester, Rochester, New York, USA

Department of Biostatistics and Computational Biology, University of Rochester School of Medicine and Dentistry, Rochester, New York, USA

Department of Biomedical Genetics, University of Rochester School of Medicine and Dentistry, Rochester, New York, USA

Department of Biochemistry & Biophysics and Center for RNA Biology, University of Rochester Medical Center, Rochester, New York, USA

Terry Zhou and Nora J. Gilliam contributed equally. Author order was determined by the initiation of the project and drafting of the manuscript. Sizhen Li and Simone Spandau contributed equally. Author order was determined in the order of decreasing seniority.

ABSTRACT Defective viral genomes (DVGs) have been identified in many RNA viruses as a major factor influencing antiviral immune response and viral pathogenesis. However, the generation and function of DVGs in SARS-CoV-2 infection are less known. In this study, we elucidated DVG generation in SARS-CoV-2 and its relationship with host antiviral immune response. We observed DVGs ubiquitously from transcriptome sequencing (RNA-seq) data sets of in vitro infections and autopsy lung tissues of COVID-19 patients. Four genomic hot spots were identified for DVG recombination, and RNA secondary structures were suggested to mediate DVG formation. Functionally, bulk and single-cell RNA-seq analysis indicated the interferon (IFN) stimulation of SARS-CoV-2 DVGs. We further applied our criteria to the next-generation sequencing (NGS) data set from a published cohort study and observed a significantly higher amount and frequency of DVG in symptomatic patients than those in asymptomatic patients. Finally, we observed exceptionally diverse DVG populations in one immunosuppressive patient up to 140 days after the first positive test of COVID-19, suggesting for the first time an association between DVGs and persistent viral infections in SARS-CoV-2. Together, our findings strongly suggest a critical role of DVGs in modulating host IFN responses and symptom development, calling for further inquiry into the mechanisms of DVG generation and into how DVGs modulate host responses and infection outcome during SARS-CoV-2 infection.

IMPORTANCE Defective viral genomes (DVGs) are generated ubiquitously in many RNA viruses, including SARS-CoV-2. Their interference activity to full-length viruses and IFN stimulation provide the potential for them to be used in novel antiviral therapies and vaccine development. SARS-CoV-2 DVGs are generated through the recombination of two discontinuous genomic fragments by viral polymerase complex, and this recombination is also one of the major mechanisms for the emergence of new coronaviruses. Focusing on the generation and function of SARS-CoV-2 DVGs, these studies identify new hot spots for nonhomologous recombination and strongly suggest that the secondary structures within viral genomes mediate the recombination. Furthermore, these studies provide the first evidence for IFN stimulation activity of de novo DVGs during natural SARS-CoV-2 infection. These findings set up the foundation for further mechanism studies of SARS-CoV-2 recombination and provide evidence to harness the immunostimulatory potential of DVGs in the development of a vaccine and antivirals for SARS-CoV-2.

Invited Editor Matthew B. Frieman, University of Maryland School of Medicine Editor Diane E. Griffin, Johns Hopkins Bloomberg School of Public Health Copyright © 2023 Zhou et al. This is an openacross article distributed under the terms of

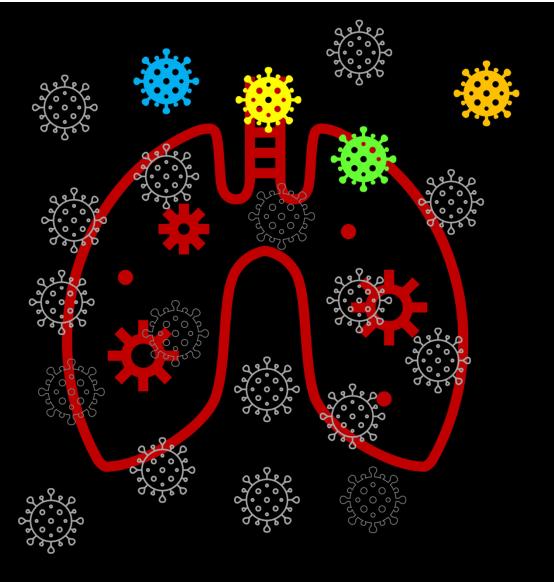
access article distributed under the terms of the Creative Commons Attribution 4.0 International license, Address correspondence to Yan Sun,

Address correspondence to Yan Sun, Yan_Sun@URMC.Rochester.edu. The authors declare no conflict of interest

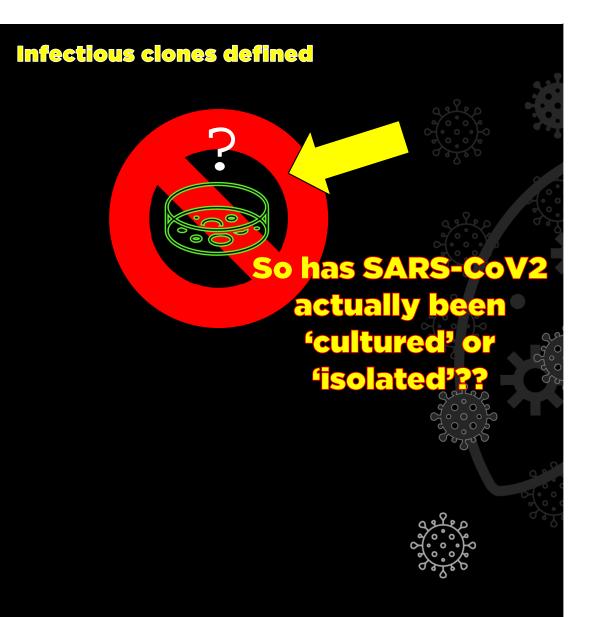
Received 1 February 2023 Accepted 28 March 2023

Month YYYY Volume XX Issue XX 10.1128/mbio.00250-23 1

Infectious clones defined



Infectious clones defined



Clinical Infectious Diseases

CORRESPONDENCE





Correlation Between 3790 Quantitative Polymerase Chain Reaction-Positives Samples and Positive Cell Cultures, Including 1941 Severe Acute Respiratory Syndrome Coronavirus 2 Isolates

To the Editor-The outbreak of the coronavirus disease 2019 (COVID-19) pandemic due to severe acute respiratory syndrome coronavirus 2 (SARS-CoV-2) was declared a pandemic on 12 March 2020 by the World Health Organization [1]. A major issue related to the outbreak has been to correlate viral RNA load obtained after reverse-transcription polvmerase chain reaction (RT-PCR) and expressed as the cycle threshold (Ct) with contagiousness and therefore duration of eviction from contacts and discharge from specialized infectious disease

wards. Several recent publications, based | RT-PCR for 179 151 patients, of whom on more than 100 studies, have attempted to propose a cutoff Ct value and duration of eviction, with a consensus at approximately Ct >30 and at least 10 days, respectively [2-5]. However, in an article published in Clinical Infectious Diseases, Bullard et al reported that patients could not be contagious with Ct >25 as the virus is not detected in culture above this value [6]. This limit was then evoked in the French media during an interview with a member of the French Scientific Council Covid-19 as a possible value above which patients are no longer contagious [7].

At the beginning of the outbreak, we correlated Ct values obtained using our PCR technique based on amplification of the E gene and the results of the culture [8]. Since the beginning of the pandemic, we have performed 250 566 SARS-CoV-2

13 161 (7.3%) tested positive. Up to the end of May, 3790 of these samples, reported as positive on nasopharyngeal samples, were inoculated and managed for culture as previously described [8]. Of these 3790 inoculated samples, 1941 SARS-CoV-2 isolates could be obtained after the first inoculation or up to 2 blind subcultures. The correlation between the scanner values and the positivity of the culture allows us to observe that the image obtained with 10 times more isolates than in our preliminary work (1941 vs 129) does not change significantly (Figure 1). It can be observed that at Ct = 25, up to 70% of patients remain positive in culture and that at Ct = 30this value drops to 20%. At Ct = 35, the value we used to report a positive result for PCR, <3% of cultures are positive. Our Ct value of 35, initially based on the results

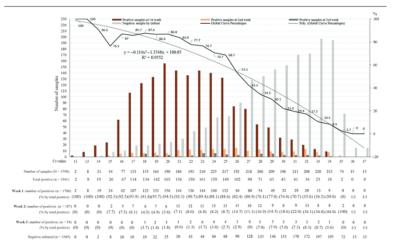
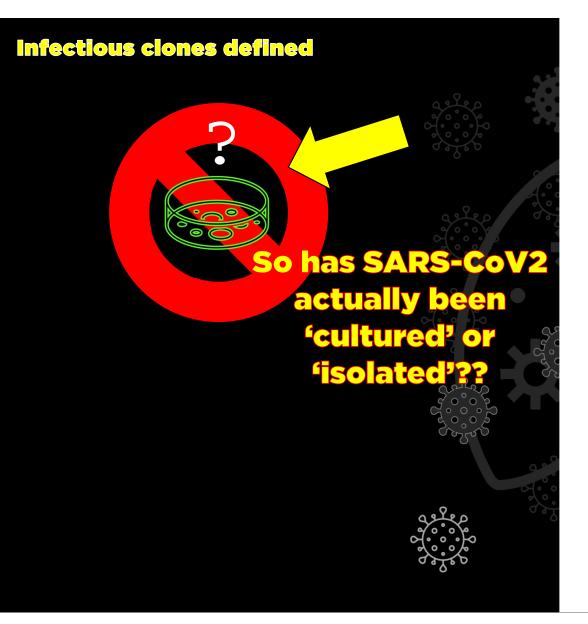


Figure 1. Percentage of positive viral cultures of severe acute respiratory syndrome coronavirus 2 polymerase chain reaction-positive nasopharyngeal samples from coronavirus disease 2019 patients, according to Ct value (plain line). The dashed curve indicates the polynomial regression curve. Abbreviations: Ct, cycle threshold; Poly, polynomial.

e932 • CID 2021:72 (1 June) • CORRESPONDENCE



BRIEF REPORT



Viral RNA load as determined by cell culture as a management tool for discharge of SARS-CoV-2 patients from infectious disease wards

Bernard La Scola ^{1,2} . • Marion Le Bideau ^{1,2} • Julien Andreani ^{1,2} • Van Thuan Hoang ^{1,3,4} • Clio Grimaldier ^{1,2} • Philippe Colson ^{1,2} • Philippe Gautret ^{1,3} • Didier Raoult ^{1,2}

Received: 31 March 2020 / Accepted: 21 April 2020 / Published online: 27 April 2020 © The Author(s) 2020

Abstract

In a preliminary clinical study, we observed that the combination of hydroxychloroquine and azithromycin was effective against SARS-CoV-2 by shortening the duration of viral load in Covid-19 patients. It is of paramount importance to define when a treated patient can be considered as no longer contagious. Correlation between successful isolation of virus in cell culture and Ct value of quantitative RT-PCR targeting E gene suggests that patients with Ct above 33–34 using our RT-PCR system are not contagious and thus can be discharged from hospital care or strict confinement for non-hospitalized patients.

Keywords SARS-CoV2 · Covid-19 · RT-PCR · Co-culture · Viral load · Correlation

Introduction

An outbreak of an emerging disease (Covid-19) due to SARS-CoV-2 started in Wuhan, China, then rapidly spread in China, and was declared pandemic on March 12, 2020, by the WHO [1-3]. Currently, the overall case fatality rate is about 2.3% in China, which is likely an overestimate because most patients have mild symptoms and are thus not tested [4]. Because of a study showing that chloroquine and hydroxychloroquine inhibit SARS-CoV-2 in vitro, we tested hydroxychloroquine as a treatment in Covid-19 patients [5, 6]. Our results show that in treated patients, the nasopharyngeal viral load of SARS-CoV-2-infected patients was cleared in only 3 to 6 days. Our results also suggest a synergistic effect of the combination of hydroxychloroquine and azithromycin, two molecules previously demonstrated to be active in vitro against Zika and

- ☑ Bernard La Scola bernard.la-scola@univ-amu.fr
- ☑ Didier Raoult didier.raoult@gmail.com
- ¹ IHU-Méditerranée Infection, Marseille, France
- Aix Marseille Univ, IRD, APHM, MEPHI, Marseille, France
- ³ Aix Marseille Univ, IRD, AP-HM, SSA, VITROME, Marseille, France
- Thai Binh University of Medicine and Pharmacy, Thai Binh, Viet

Ebola viruses [7–10] and to prevent severe respiratory tract infections when administered to patients suffering viral infection [11]. These results are of great importance because a recent paper has shown that the median duration of viral RNA detection in patients suffering from Covid-19 in China was 20 days, with the longest duration being 37 days [12]. We are now facing a massive influx of patients in need of treatment and hospitalization, ideally in infectious disease wards equipped with NSB3 modules with negative pressure. Thus, in addition to obtaining complete disappearance of virus RNA in respiratory samples, having a PCR-based indicator of loss of contagiousness is a major priority for discharge from infectious diseases ward. Based on a set of 183 samples from 155 patients, we observed a significant relationship between viral RNA load and culture positivity.

The Méditerranée Infection University Hospital Institute in Marseille is the reference center for highly infectious diseases for Southeastem France. It was the only center in this region with diagnostic tests available during the first weeks of the epidemic in France and received patients' samples from this whole area. From the day of the first positive test, on February 27 until March 12, 4384 clinical samples were tested by RT-PCR for 3466 patients. Since the beginning of this crisis and until now, on March 26, we inoculated 1049 samples and could obtain in culture 611 SARS-CoV-2 isolates. A total of 183 samples testing positive by RT-PCR, including 9 sputum samples and 174 naso-pharyngeal swabs from 155 patients, were inoculated in cell cultures. SARS-CoV-2 RNA positivity in patient samples waples and 174 naso-pharyngeal swabs from 155 patients, were inoculated in cell cultures. SARS-CoV-2 RNA positivity in patient samples waples waples



Infectious clo

BRIEF REPORT



Viral RNA load as determined by cell culture as a management tool for discharge of SARS-CoV-2 patients from infectious disease wards

Bernard La Scola ^{1,2} . • Marion Le Bideau ^{1,2} • Julien Andreani ^{1,2} • Van Thuan Hoang ^{1,3,4} • Clio Grimaldier Philippe Colson ^{1,2} • Philippe Gautret ^{1,3} • Didier Raoult ^{1,2}

Received: 31 March 2020 / Accepted: 21 April 2020 / Published online: 27 April 2020 © The Author(s) 2020

Abstract

In a preliminary clinical study, we observed that the combination of hydroxychloroquine and azithromycin was ef SARS-CoV-2 by shortening the duration of viral load in Covid-19 patients. It is of paramount importance to define patient can be considered as no longer contagious. Correlation between successful isolation of virus in cell culture a quantitative RT-PCR targeting E gene suggests that patients with Ct above 33–34 using our RT-PCR system are 1 and thus can be discharged from hospital care or strict confinement for non-hospitalized patients.

Keywords SARS-CoV2 · Covid-19 · RT-PCR · Co-culture · Viral load · Correlation

Introduction

An outbreak of an emerging disease (Covid-19) due to SARS-CoV-2 started in Wuhan, China, then rapidly spread in China, and was declared pandemic on March 12, 2020, by the WHO [1–3]. Currently, the overall case fatality rate is about 2.3% in China, which is likely an overestimate because most patients have mild symptoms and are thus not tested [4]. Because of a study showing that chloroquine and hydroxychloroquine inhibit SARS-CoV-2 in vitro, we tested hydroxychloroquine as a treatment in Covid-19 patients [5, 6]. Our results show that in treated patients, the nasopharyngeal viral load of SARS-CoV-2-infected patients was cleared in only 3 to 6 days. Our results also suggest a synergistic effect of the combination of hydroxychloroquine and azithromycin, two molecules previously demonstrated to be active in vitro against Zika and

- ¹ IHU-Méditerranée Infection, Marseille, France
- Aix Marseille Univ, IRD, APHM, MEPHI, Marseille, France
- ³ Aix Marseille Univ, IRD, AP-HM, SSA, VITROME, Marseille, France
- Thai Binh University of Medicine and Pharmacy, Thai Binh, Viet Nam

Ebola viruses [7–10] and to prevent severe re infections when administered to patients sufferi tion [11]. These results are of great importar recent paper has shown that the median dur RNA detection in patients suffering from Covi was 20 days, with the longest duration being 37 are now facing a massive influx of patients in ment and hospitalization, ideally in infectious equipped with NSB3 modules with negative p in addition to obtaining complete disappearance in respiratory samples, having a PCR-based in of contagiousness is a major priority for dischartious diseases ward. Based on a set of 183 sam patients, we observed a significant relationship RNA load and culture positivity.

The Méditerranée Infection University Hosp
Marseille is the reference center for highly info
for Southeastern France. It was the only center in this region with
diagnostic tests available during the first weeks of the epidemic
in France and received patients' samples from this whole area.
From the day of the first positive test, on February 27 until
March 12, 4384 clinical samples were tested by RT-PCR for
3466 patients. Since the beginning of this crisis and until now,
on March 26, we inoculated 1049 samples and could obtain in
culture 611 SARS-CoV-2 isolates. A total of 183 samples testing
positive by RT-PCR, including 9 sputum samples and 174 nasopharyngeal swabs from 155 patients, were inoculated in cell
cultures. SARS-CoV-2 RNA positivity in patient samples was

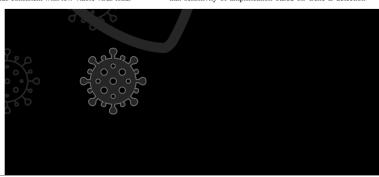


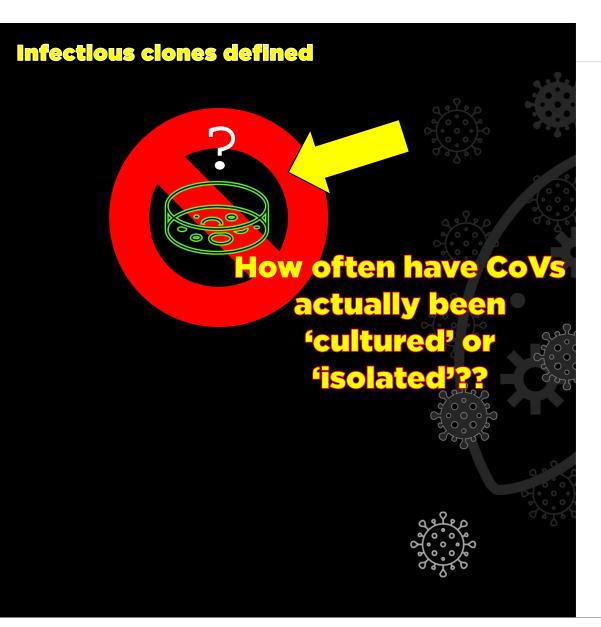
Eur J Clin Microbiol Infect Dis (2020) 39:1059–1061

assessed by real-time reverse transcription-PCR targeting the E gene, as previously described [13]. For all patients, 500 µL of nasopharyngeal swab fluid (Virocult, Elitech, France) or sputum sample were passed through 0.22-um pore sized centrifugal filter (Merck Millipore, Darmstadt, Germany) and then were inoculated in 4 wells of 96-well culture microplates containing Vero E6 cells (ATCC CRL-1586) into Minimum Essential Medium culture medium with 4% fetal calf serum and 1% glutamine. All samples were inoculated between 4 and 10 h after sampling and kept at +4 °C before processing. After centrifugation at $4000 \times g$, microplates were incubated at 37 °C. They were observed daily for evidence of cytopathogenic effect. Two subcultures were performed weekly. Presumptive detection of virus in supernatant showing cytopathic effect was done using the SU5000 scanning electron microscope (Hitachi High-Tech Corporation, Tokyo, Japan) and then confirmed by specific RT-PCR targeting E gene. Variation of culture positivity rate was assessed statistically as the proportion of variance explained by Ct value and considered adequately fitted if the coefficient of determination (R² statistic) was > 50%

Among the 183 samples inoculated in the studied period of time, 129 led to virus isolation. Of these, 124 samples had detectable cytopathic effect between 24 and 96 h. Blind subcultures allowed obtaining 5 additional isolates only. We observed a significant relationship between Ct value and culture positivity rate (Fig. 1). Samples with Ct values of 13–17 all led to positive culture. Culture positivity rate then decreased progressively according to Ct values to reach 12% at 33 Ct. No culture was obtained from samples with Ct ≥ 34. The 5 additional isolates obtained after blind subcultures had Ct between 27 and 34, thus consistent with low viable virus load.

In the present work, we observe a strong correlation between Ct value and sample infectivity in a cell culture model. On the basis of this data, we can deduce that with our system, patients with Ct values equal or above 34 do not excrete infectious viral particles. It was observed that SARS-CoV-2 was detected up to 20 days after onset of symptoms by PCR in infected patients but that the virus could not be isolated after day 8 in spite of ongoing high viral loads of approximately 10^5 RNA copies/mL of sample, using the RT-PCR system used in the present study [14]. Progressive decrease of viral load over time is observed in all studies conducted in Covid-19 patients with positive detection being observed until 17-21 days after onset of symptoms, independently of symptoms [15]. These previous observations suggested that isolation of patients after diagnosis was mandatory. However, due to prolonged shedding of RNA in respiratory samples, the criteria for ending the isolation of a patient were not clear, and there was a need to correlate viral load to cultivable viruses. Our results show that in our system of RT-PCR, we can assess that patients with Ct equal or above 34 may be discharged. In 6 patients under the current therapeutic protocol used at our institute (hydroxychloroquine and azithromycin), Ct values > 34 were obtained between days 2 and 4 post-treatment [6]. There is no previous correlation demonstrated between level viral load in respiratory samples and infectivity. However, this reduction is the basis of all procedures used for the validation of disinfectants [16]. One limitation of our work is that it cannot be extrapolated to other hospital centers since they use different systems of sample transport, of RNA extraction, and of PCR with different primers and probes: i.e. it has been suggested that sensitivity of amplification based on Gene E detection





BMC Infectious Diseases



Research article

Open Access

A novel pancoronavirus RT-PCR assay: frequent detection of human coronavirus NL63 in children hospitalized with respiratory tract infections in Belgium

Elien Moës¹, Leen Vijgen¹, Els Keyaerts¹, Kalina Zlateva¹, Sandra Li¹, Piet Maes¹, Krzysztof Pyrc², Ben Berkhout², Lia van der Hoek² and Marc Van Ranst*¹

Address: ¹Laboratory of Clinical & Epidemiological Virology, Department of Microbiology & Immunology, Rega Institute for Medical Research, University of Leuven, Belgium and ²Department of Human Retrovirology, Academic Medical Center, University of Amsterdam, ⁷The Netherlands

Email: Elien Moës - elien.moes@uz.kuleuven.ac.be; Leen Vijgen - leen.vijgen@uz.kuleuven.ac.be; Els Keyaerts - els.keyaerts@uz.kuleuven.ac.be; Kalina Zlateva - kalina.zlateva@uz.kuleuven.ac.be; Sandra.li@uz.kuleuven.ac.be; Piet Maes - piet.3.maes@uz.kuleuven.ac.be; Kzysztof Pyrc - k.a.pyrc@amc.uva.nl; Ben Berkhout - b.berkhout@amc.uva.nl; Lia van der Hoek - c.m.vanderhoek@amc.uva.nl; Marc Van Ranst * - marc.vanrans@uz.kuleuven.ac.be

* Corresponding author

Published: 01 February 2005

Received: 13 October 2004 Accepted: 01 February 2005

BMC Infectious Diseases 2005, 5:6 doi:10.1186/1471-2334-5-6

This article is available from: http://www.biomedcentral.com/1471-2334/5/6

This is an Open Access article distributed under the terms of the Creative Commons Attribution License (http://creativecommons.org/licenses/by/2.0), which permits unrestricted use, distribution, and reproduction in any medium, provided the original work is properly cited.

Abstract

© 2005 Moës et al: licensee BioMed Central Ltd.

Background: Four human coronaviruses are currently known to infect the respiratory tract: human coronaviruses OC43 (HCoV-OC43) and 229E (HCoV-229E), SARS associated coronavirus (SARS-CoV) and the recently identified human coronavirus NL63 (HCoV-NL63). In this study we explored the incidence of HCoV-NL63 infection in children diagnosed with respiratory tract infections in Belvium.

Methods: Samples from children hospitalized with respiratory diseases during the winter seasons of 2003 and 2004 were evaluated for the presence of HCoV-NL63 using a optimized pancoronavirus RT-PCR assay.

Results: Seven HCoV-NL63 positive samples were identified, six were collected during January/ February 2003 and one at the end of February 2004.

Conclusions: Our results support the notation that HCoV-NL63 can cause serious respiratory symptoms in children. Sequence analysis of the S gene showed that our isolates could be classified into two subtypes corresponding to the two prototype HCoV-NL63 sequences isolated in The Netherlands in 1988 and 2003, indicating that these two subtypes may currently be cocirculating.

Background

Coronaviruses are large, enveloped, positive stranded RNA-viruses [1]. The viral RNA genome is 27–32 kb in size, capped, polyadenylated and encapsidated in a helical nucleocapsid. The envelope is studded with long, petalshaped spikes, giving the virus particle a characteristic crown-like appearance. Three distinct groups of coronaviruses have been described based on serological affinity and genome sequence. Coronaviruses can infect humans and a variety of domestic animals and can cause highly

Page 1 of 10 (page number not for citation purposes)





1

A Pancoronavirus RT-PCR Assay for Detection of All Known Coronaviruses

Leen Vijgen, Elien Moës, Els Keyaerts, Sandra Li, and Marc Van Ranst

Abstract

The recent discoveries of novel human coronaviruses, including the coronavirus causing SARS, and the previously unrecognized human coronaviruses HCoV-NL63 and HCoV-HKU1, indicate that the family *Coronaviridae* harbors more members than was previously assumed. All human coronaviruses characterized at present are associated with respiratory illnesses, ranging from mild common colds to more severe lower respiratory tract infections. Since the etiology of a relatively large percentage of respiratory tract diseases remains unidentified, it is possible that for a certain number of these illnesses, a yet unknown viral causative agent may be found. Screening for the presence of novel coronaviruses requires the use of a method that can detect all coronaviruses known at present. In this chapter, we describe a pancoronavirus degenerate primer-based method that allows the detection of all known and possibly unknown coronaviruses by RT-PCR amplification and sequencing of a 251-bp fragment of the coronavirus polymerase gene.

Key words: coronavirus; pancoronavirus RT-PCR; degenerate primers; sequencing; polymerase gene

1. Introduction

At present, viral culture is the "gold standard" for laboratory diagnosis of respiratory infections. Since coronaviruses are very difficult to grow in cell culture, accurate and sensitive diagnoses are not feasible by this technique. To overcome the lack of sensitivity and to obtain rapid diagnostic results, more sensitive molecular methods for the detection of human coronaviruses (HCoVs) have been developed, including reverse-transcriptase polymerase chain reaction

From: Methods in Molecular Biology, vol. 454: SARS- and Other Coronaviruses, Edited by: D. Cavanagh, DOI: 10.1007/978-1-59745-181-9_1, © Humana Press, New York, NY

Diseases



Open Access

-PCR assay: frequent detection of 1 children hospitalized with respiratory

(eyaerts¹, Kalina Zlateva¹, Sandra Li¹, Berkhout², Lia van der Hoek² and Marc Van

y, Department of Microbiology & Immunology, Rega Institute for Medical Research, Retrovirology, Academic Medical Center, University of Amsterdam, The Netherlands

ljgen - leen.vijgen@uz.kuleuven.ac.be; Els Keyaerts - els.keyaerts@uz.kuleuven.ac.be; Li - sandra.li@uz.kuleuven.ac.be; Piet Maes - piet.3.maes@uz.kuleuven.ac.be; khout@amc.uva.ni; Lia van der Hoek - c.m.vanderhoek@amc.uva.ni; Marc Van

> Received: 13 October 2004 Accepted: 01 February 2005

171-2334/5/6

he Creative Commons Attribution License (http://creativecommons.org/licenses/by/2.0), in any medium, provided the original work is properly cited.

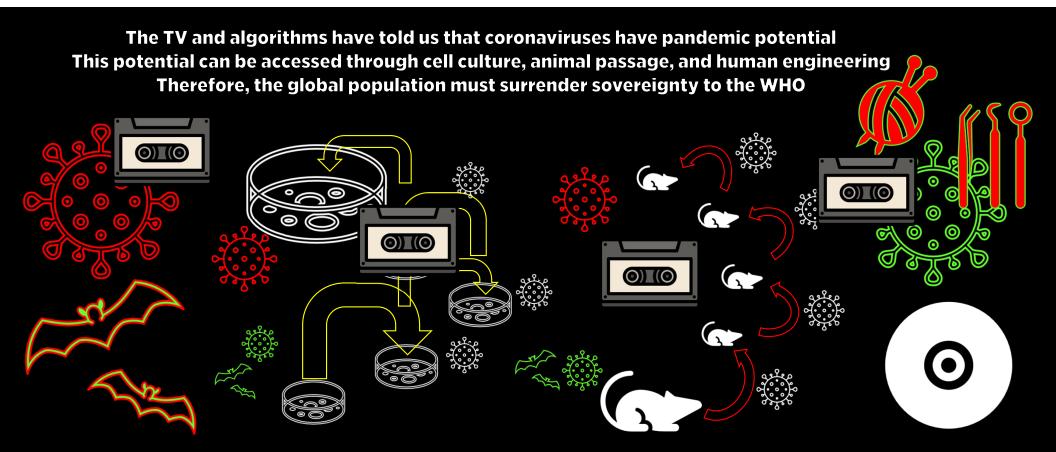
iruses are currently known to infect the respiratory tract: OC43) and 229E (HCoV-229E), SARS associated coronavirus ad human coronavirus NL63 (HCoV-NL63). In this study we L63 infection in children diagnosed with respiratory tract

ipitalized with respiratory diseases during the winter seasons d for the presence of HCoV-NL63 using a optimized

samples were identified, six were collected during January/ February 2004.

he notation that HCoV-NL63 can cause serious respiratory rsis of the S gene showed that our isolates could be classified the two prototype HCoV-NL63 sequences isolated in The ting that these two subtypes may currently be cocirculating.

stranded 32 kb in 1a helical 1g. petalshaped spikes, giving the virus particle a characteristic crown-like appearance. Three distinct groups of coronaviruses have been described based on serological affinity and genome sequence. Coronaviruses can infect humans and a variety of domestic animals and can cause highly



To coerce a surrender of individual sovereignty and a global fundamental inversion of human rights from freedom to fascism

■ TO TAL DEATHS

NUM COVID-19 DEATHS

NUM PNEUMONIA DEATHS

NUM INFLUENZA DEATHS

₁₀ Hypothesis:

The WHO declared a pandemic of a DANGEROUS NOVEL virus—said to be detectable by non-specific PCR test for RNA viruses applied to low prevalence populations (high percentage false positives, endemic background signal) and intentionally correlated with poor or detrimental health protocols through financial incentives—that enabled a larger percentage of all cause mortality than PnI (pneumonia and influenza) to be prioritized as a national security threat composed of vaccine preventable deaths. The US was ready with a plan to respond to a coronavirus pandemic, and that plan is in motion.

A NIAID funded infectious DNA/RNA infectious clone of a CoV may or may not be involved in the initial biological incident(s), but a natural CoV swarm cannot sustain a pandemic.

The goal is the total surrender of individual sovereignty and enforcement of a global fundamental inversion from basic human rights to basic granted

permissions

https://www.researchgate.net/publication/362427136

Figure 1 shows the all-cause mortality by month (ACM/m) for the USA from January 1999 to December 2021.

So millions of doses didn't change all cause mortality?

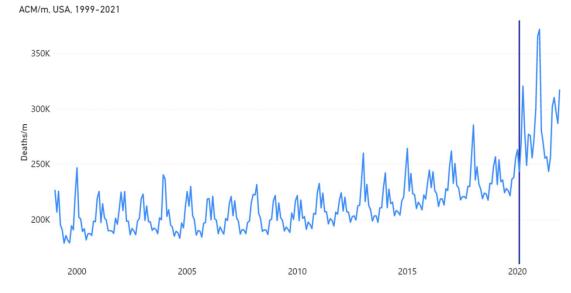


Figure 1. All-cause mortality by month in the USA from 1999 to 2021. Data are displayed from January 1999 to December 2021. The vertical dark-blue line indicates the month of February 2020, intended to point the beginning of the covid period. Data were retrieved from CDC (CDC, 2022a), as described in Table 1.

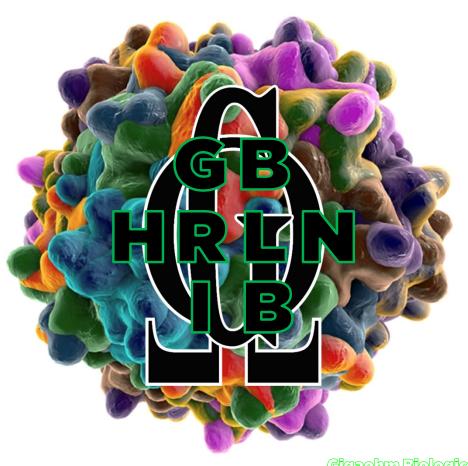
Poverty level
Household income
Serious mental-illness
Obesity
and the excess mortality is a direct
correlation across states

True with and without vaccines
Not correlated with age?!

This means that it cannot be from a CoV because there is an exponential relationship between age and CoV infection fatality







Gigaohm Biological High Resistance Low Noise Information Brief 23 April 2023

https://www/ncbin/m nih gov/pm c/articles Pros @ 师97082/ **EXPERIMENTAL EVOLUTION** CYTOLYTIC. PERSISTENT. **ADAPTATION TO** CLONAL INFECTIONS **ALTERNATIVE HOST VIRUS** SAMPLE SELECTIVE PLAQUE-TO-PLAQUE TRANSFERS

Fig 3. Scope of viral population dynamics. Upon isolation from an infected host (middle boxes), a virus sample may be adapted to cultured cells and subjected to large population or bottleneck transfers (left box), or be adapted to a different host in vivo (right box). Relevant adaptive mutations are highlighted with colored symbols.

https://doi.org/10.1371/journal.pgen.1008271.g003

Each natural infection is a unique bottleneck. Each im m unized infection is NOT a unique bottleneck.

TOPIC PAGE

Viral quasispecies

Esteban Domingo 1,2, Celia Perales 1,2,3

- 1 Centro de Biología Molecular Severo Ochoa (CSIC-UAM), Consejo Superior de Investigaciones Científicas (CSIC), Campus de Cantoblanco, Madrid, Spain, 2 Centro de Investigación Biomédica en Red de Enfermedades Hepáticas y Digestivas (CIBERPahd) del Instituto de Salud Carlos III, Madrid, Spain, 3 Department of Clinical Microbiology, IIS-Fundación Jiménez Díaz, UAM, Madrid, Spain,
- * edomingo@cbm.csic.es

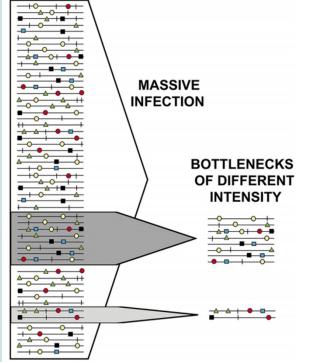


Fig 4. Illustration of bottleneck of different severity, defined by the different arrows acting on the entire populatio. Symbols represent mutation types.

term replicon to that link fe [1,2]. The theated by a master he distribution. It nasizing the relee constraints. One

Schuster to

ely large numit clouds. Fueled ve frequency as ory of the origin of

experimentally

onal analyses ads of mutant . The quasispewhen the genome uses, ubiquitous

, quasispecies

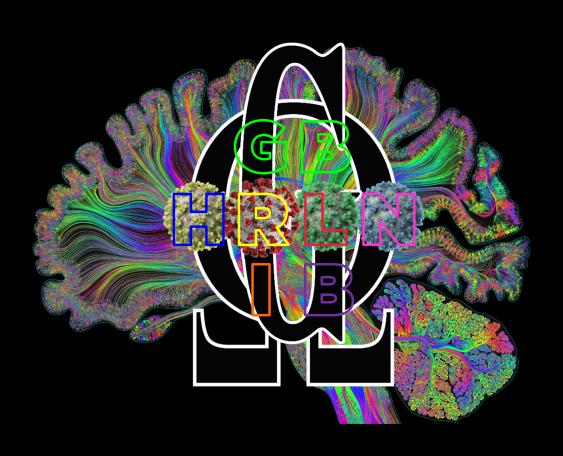
bjected to genetic

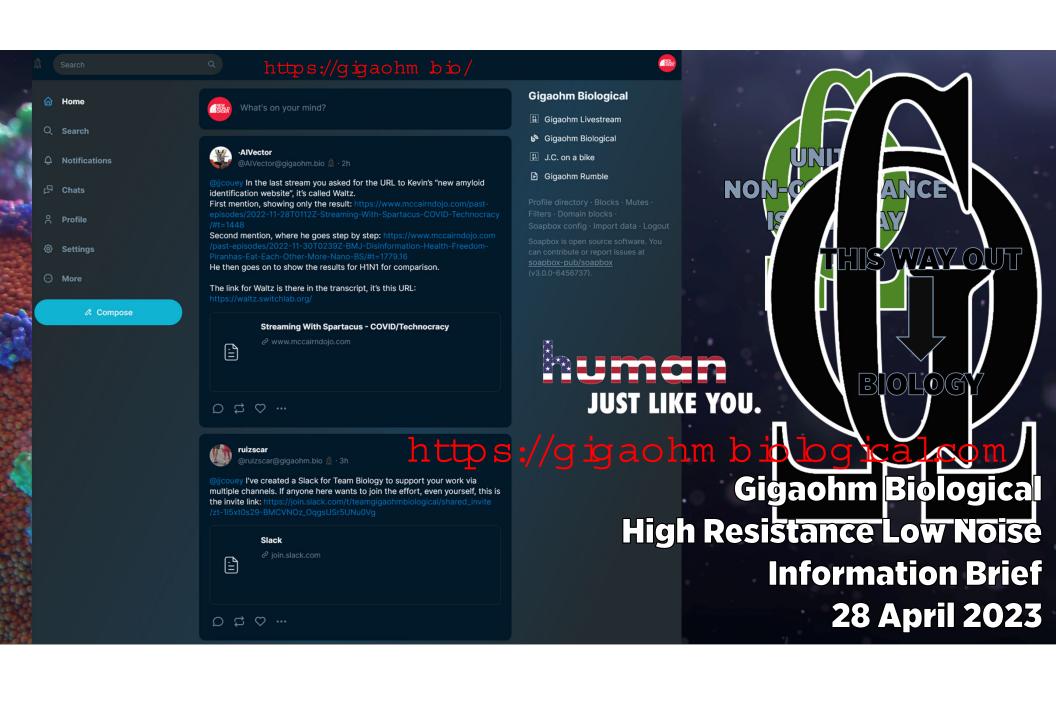
. Despite being compatible with

a transition that

type, and a conruses that con-

https://doi.org/10.1371/journal.pgen.1008271.g004







HHS Public Access

Author manuscript

Science. Author manuscript; available in PMC 2017 May 11.

Published in final edited form as:

Science. 2016 November 11; 354(6313): 722-726. doi:10.1126/science.aag1322.

Potent Protection against H5N1 and H7N9 Influenza via Childhood Hemagglutinin Imprinting*

Katelyn M. Gostic 1, Monique Ambrose 1, Michael Worobey 2,** , and James O. Lloyd-Smith 1,3,**

¹Department of Ecology and Evolutionary Biology, University of California, Los Angeles, Los Angeles, CA, 90095, USA

²Department of Ecology and Evolutionary Biology, University of Arizona, Tucson, AZ, 85721, USA

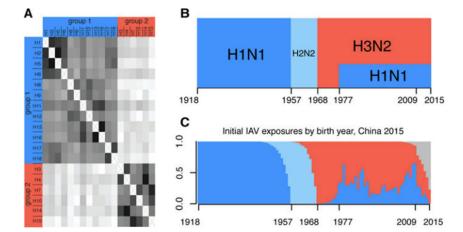
³Fogarty International Center, National Institutes of Health, Bethesda, MD, 20892, USA

Abstract

Two zoonotic influenza A viruses (IAV) of global concern, H5N1 and H7N9, exhibit unexplained differences in age distribution of human cases. Using data from all known human cases of these viruses, we show that an individual's first IAV infection confers lifelong protection against severe disease from novel hemagglutinin (HA) subtypes in the same phylogenetic group. Statistical modeling shows protective HA imprinting is the crucial explanatory factor, providing 75% protection against severe infection and 80% protection against death for both H5N1 and H7N9. Our results enable us to predict age distributions of severe disease for future pandemics and demonstrate that a novel strain's pandemic potential increases yearly when a group-mismatched HA subtype dominates seasonal influenza circulation. These findings open new frontiers for rational pandemic risk assessment.

The spillover of novel influenza A viruses (IAV) is a persistent threat to global health. H5N1 and H7N9 are particularly concerning avian-origin IAVs, each having caused hundreds of severe or fatal human cases (1). Despite commonalities in their reservoir hosts and epidemiology, these viruses show puzzling differences in age distribution of observed human cases (1,2). Existing explanations, including possible protection against H5N1 among older birth-year cohorts exposed to the neuraminidase of H1N1 as children (3,4) or age biases in exposure to infected poultry (5–7), cannot fully explain these opposing patterns of severe disease and mortality. Another idea is that severity of H5N1 and H7N9 differs by age, leading to case ascertainment biases (1), but no explanatory mechanism has been proposed.

Figures S1–S12 Tables S1–S2 Databases S1–S3 References (35–74)



https://www.ncbinlm.nih.gov/labs/pm.c/articles/PMC5134739/

Fig. 1.

HA groups and reconstruction of 20th century HA imprinting. (A) HA groups 1 and 2, and pairwise amino acid similarities in the HA stem region. Darker colored cells indicate higher similarity (see Fig. S1). Each within-group subtype pair is more similar (83.2%–97.8%) than any between-group pair (75.9%–81.7%). (B) History of seasonal IAV circulation, and (C) estimated fraction of each birth cohort in China with initial exposure to each subtype. Estimated patterns in other countries (not shown) are identical up to 1977, and very similar thereafter. Pandemic years are marked on the horizontal axis. Blue represents group 1 HA viruses, red represents group 2, and grey represents naïve children who have not yet experienced an IAV infection.

^{*}This manuscript has been accepted for publication in Science. This version has not undergone final editing. Please refer to the complete version of record at http://www.sciencemag.org/. The manuscript may not be reproduced or used in any manner that does not fall within the fair use provisions of the Copyright Act without the prior, written permission of AAAS.

[&]quot;Correspondence and requests for materials should be addressed to worobey@email.arizona.edu or jlloydsmith@ucla.edu. The authors declare no competing financial interests.



HHS Public Access

Author manuscript

Science. Author manuscript; available in PMC 2017 May 11.

Published in final edited form as:

Science. 2016 November 11; 354(6313): 722-726. doi:10.1126/science.aag1322.

Potent Protection against H5N1 and H7N9 Influenza via Childhood Hemagglutinin Imprinting*

Katelyn M. Gostic 1, Monique Ambrose 1, Michael Worobey 2,** , and James O. Lloyd-Smith 1,3,**

¹Department of Ecology and Evolutionary Biology, University of California, Los Angeles, Los Angeles, CA, 90095, USA

²Department of Ecology and Evolutionary Biology, University of Arizona, Tucson, AZ, 85721, USA

³Fogarty International Center, National Institutes of Health, Bethesda, MD, 20892, USA

Abstract

Two zoonotic influenza A viruses (IAV) of global concern, H5N1 and H7N9, exhibit unexplained differences in age distribution of human cases. Using data from all known human cases of these viruses, we show that an individual's first IAV infection confers lifelong protection against severe disease from novel hemagglutinin (HA) subtypes in the same phylogenetic group. Statistical modeling shows protective HA imprinting is the crucial explanatory factor, providing 75% protection against severe infection and 80% protection against death for both H5N1 and H7N9. Our results enable us to predict age distributions of severe disease for future pandemics and demonstrate that a novel strain's pandemic potential increases yearly when a group-mismatched HA subtype dominates seasonal influenza circulation. These findings open new frontiers for rational pandemic risk assessment.

The spillover of novel influenza A viruses (IAV) is a persistent threat to global health. H5N1 and H7N9 are particularly concerning avian-origin IAVs, each having caused hundreds of severe or fatal human cases (1). Despite commonalities in their reservoir hosts and epidemiology, these viruses show puzzling differences in age distribution of observed human cases (1,2). Existing explanations, including possible protection against H5N1 among older birth-year cohorts exposed to the neuraminidase of H1N1 as children (3,4) or age biases in exposure to infected poultry (5–7), cannot fully explain these opposing patterns of severe disease and mortality. Another idea is that severity of H5N1 and H7N9 differs by age, leading to case ascertainment biases (1), but no explanatory mechanism has been proposed.

Figures S1–S12 Tables S1–S2 Databases S1–S3

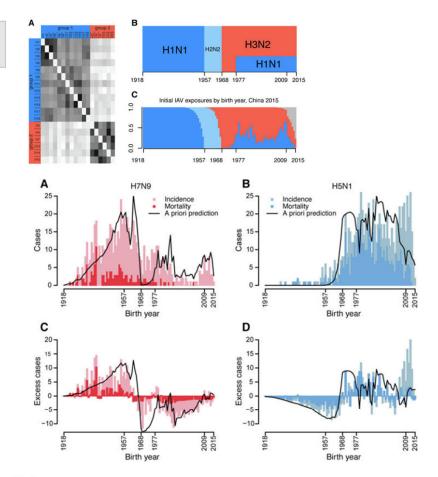
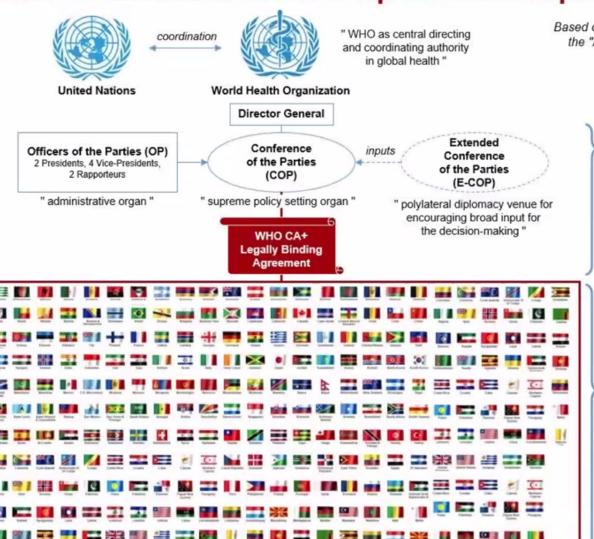


Fig. 2.
H7N9 and H5N1 observed cases and deaths by birth year (bars). Black lines show *a priori* prediction based on demographic age distribution and reconstructed patterns of HA imprinting. (A) 680 H7N9 cases, from China, 2013–2015. (B) 835 H5N1 cases, from Cambodia, China, Egypt, Indonesia, Thailand and Vietnam, 1997–2015. (C, D) Case data normalized to demographic age distribution from appropriate countries and case observation years.

^{*}This manuscript has been accepted for publication in Science. This version has not undergone final editing. Please refer to the complete version of record at http://www.sciencemag.org/. The manuscript may not be reproduced or used in any manner that does not fall within the fair use provisions of the Copyright Act without the prior, written permission of AAAS.

[&]quot;Correspondence and requests for materials should be addressed to worobey@email.arizona.edu or jlloydsmith@ucla.edu. The authors declare no competing financial interests.





Based on Conceptual Zero Draft of the WHO CA+, the "Agreement on Pandemic Prevention and

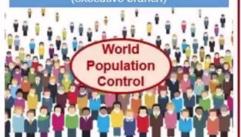
he "Agreement on Pandemic Prevention and Preparedness and Response" of 25 November 2022

> web : tinsy.me/b8TKJL pdf : urlis.net/r9qi8sb

WHO CA+ Governing Body (legislative & iudicative branches)

Decides and dictates health policies, science, definitions, emergencies, lockdowns, masks, diagnostics, tests, quarantines, certificates, products, vaccines, therapeutics, number of mandatory vaccinations, use of personnel, logistics, communications and other resources in ALL aspects of human health in every nation

National Health Authorities (executive branch)



What changes for my country and my government?

WHO CA+

establishes a new global dictatorial power architecture to dictate all aspects of human life on earth, bypassing all legislative, executive and judicial powers of local governments and thereby undermining the sovereignty of nations and its peoples.

WHO CA+ is legally bindir for countries under threat or sanctions and disciplinary measures.

Why is WHO CA+ highly dangerous and needs to be stopped?

Decisions on all aspects of human life are taken by the "COP", a small number of unelected, unaccountable and diplomatically immune bureaucrats installed by the true holders of power and their financing masters.

